Vol. VII. No.4 Editor : B.S. Tomar October 2008

Editorial

Ever since the discovery of radioactivity by Henry Becquerel in 1896, nuclear scientists have been trying to unravel the mystery behind the forces that bind the nucleonic as well as sub-nucleonic matter together. The extensive studies on common modes of nuclear decay, such as, alpha, beta and gamma decay in the early part of the twentieth century were followed by synthesis of nuclei away from the line of stability. These studies led to the discovery of several exotic decay modes of nuclei, such as, one and two proton radioactivity, cluster radioactivity, beta delayed particles emission, double beta decay, etc., which have not yet found detailed description in the text books on nuclear and radiochemistry.

The present bulletin is an attempt to introduce the various exotic nuclear decay modes of nuclei at an elementary level. I thank Dr. A.Goswami who readily agreed to be the guest editor of this thematic bulletin. My sincere thanks are due to all the authors who despite a short notice sent in their contributions in time. I hope the articles in this bulletin will ignite the minds of our young researchers in the field of nuclear chemistry and take up research in this exciting area.

CONTENTS

Guest Editor

Dr. A. Goswami
Radiochemistry Division
Bhabha Atomic Research Centre
Trombay, Mumbai 400 085

Guest Editorial

Dr. A. Goswami

Discovery of spontaneous emission of radiation from uranium salts by Henri Becquerel in 1896 marked the beginning of a new era in science. The name radioactivity was proposed for this phenomenon by Marie Curie who, along with her husband Pierre Curie, discovered two more radioactive elements Polonium and Radium (1898). They were awarded noble prize for the discovery. Rutherford was awarded noble prize in chemistry (1908) for his study on disintegration of radioactive elements. Subsequent discovery of atomic nucleus by Rutherford and group displacement law by Soddy firmly established the nuclear origin of the - and - radioactivity. Spontaneous fission as a natural decay mode was discovered after a long time in 1940.

On the theoretical side, the puzzle of -decay was solved simultaneously by Gamow and Condon and Gurney in the year 1928 based on the quantum mechanical tunneling effect. The same theory could explain the phenomenon of spontaneous fission. The problem of conservation of statistics and the continuous spectrum of -particles could be solved by the introduction of the concept of neutrino by Pauli (1931). Incidentally, the neutrino was discovered 22 years later in 1953 by Cowan Jr and Reines. It was Fermi who established the theory of -decay by introducing the concept of weak interaction, characterized by a fundamental constant that govern the beta decay.

Since the early days, there has been a constant progress made in the accelerator technology and a large number of radioactive isotopes have been produced artificially by variety of nuclear reactions. Also there has been tremendous development in the detection of rare events, using separators and multiple detectors and sophisticated pulse processing techniques. This has led to the identifications of exotic decay modes like cluster radioactivity, one- and two proton radioactivity and beta delayed particle emissions. Three articles in this bulletin would give a brief introduction to these recent developments. Double beta decay is another kind of rare decay mode for which search is on for quite sometime. An article on this topic has been included to give an idea to the readers about the kind of research activity currently pursued in this area. An article on non-nucleonic excitations in nuclei has been included to give a glimpse of the wonder-world of particles that have been discovered by high energy nuclear physics experiments, and how the concept of quark structure of hadrons (baryons and mesons) have been able to explain the host of particles that have been discovered.

It is my privilege to thank the contributors to this volume who had readily agreed to our request, and timely submitted the articles. I would also like to thank Dr. B.S. Tomar for inviting me to be the guest editor of this volume. Finally, I hope that the readers would find the articles interesting.

Cluster Radioactivity and Related Topics

Dr. Bency John *did his M.Sc. in Physics from University of Calicut in 1984. After graduating from the 29th batch of BARC Training School in 1986 he joined the Nuclear Physics Division, BARC. He completed his PhD from Mumbai University in 1999 and Postdoctoral assignment at Texas A&M University, USA during 2000-2002. His areas of research include Experimental Low Energy Nuclear Physics in general and Nuclear Fission, heavy ion induced nuclear reactions, in particular.*

Abstract

Discovery of cluster radioactivity a quarter century ago has stimulated a rapid development of experimental and theoretical investigations of the phenomenon. Major findings of this field are reviewed briefly. Due to certain characteristics of the cold-fission of heavy nuclei and the cold-heavy-cluster formation in quasi-fission, these processes are also identified with the cluster radioactivity. Study of alpha clustering in light nuclei has enriched the field of clustering in nuclei. These aspects are also reviewed briefly.

Introduction

Discovery of radioactivity in 1896 was an epoch making event that opened up the atomic and the sub-atomic world. Since then several different forms of nuclear disintegrations have been identified, including the cluster radioactivity(1984). The discovery of cluster radioactivity from heavy nuclei is one of the important findings in nuclear physics. A quantum rearrangement of large number of nucleons from one ground state of a (A,Z) nucleon system to two ground states of the cluster(A_e, Z_e) and the daughter nucleus(A_d, Z_d) systems was discovered by Rose and Jones[1], who measured ^{14}C emission from ^{223}Ra, confirming a theoretical prediction made earlier by Sandulescu et. al [2]. A rapid development of experimental and theoretical investigations was stimulated by the discovery. The Physics and Astronomy Classification Scheme(PACS) introduced a new field-23.70 +j Heavy particle decay-for dissemination of the results.

From the early days, most familiar forms of radioactive decay are the , and decays. Some of the early nuclear models (1930) proposed that the nuclei are composed of particles and electrons, probably after observing the familiar decay channels, and this may be the first instance for invoking a cluster model for the nuclei.

With the discovery of neutrons in 1932, path was open for the liquid drop model and subsequently for the shell model using the mean field concept (1950). The early shell models excluded cluster states in the nuclei, however experimental observations compelled redevelopment of the cluster model for light nuclei (1968). The interaction potential between clusters thus developed has molecular character; the effective local potentials are like those for Van der Waal gases. Subsequent work has led to anti-symmetrized molecular dynamics model(AMD, 1996) and nuclear molecular orbital representation (1970-2007) for the nuclei. The method of AMD has been proven to be a powerful method to describe the cluster and shell model like features in general nuclei.

Recently there has been increasing interests in Bose-Einstein Condensation (BEC) of particles in nuclei [3]. The phenomenon of BEC is well known for liquid helium, and recently in dilute gases. For systems of strong interaction, pion condensation and kaon condensation have been proposed but have not been confirmed experimentally [4]. Experimental signatures for BEC of alpha particles are therefore very important. Alpha cluster states get 'activated' in low lying excited states of certain light nuclei like ^{12}C, ^{16}O and ^{20}Ne, if the binding energy of

Dr. Bency John, Nuclear Physics Division, Bhabha Atomic Research Centre, Mumbai 400 085;
E-mail: bjohn@barc.gov.in

inter-cluster relative motion is almost zero or of small positive value [5]. At cluster thresholds, precipitation of the fermions-fluid into clusters occurs, and due to interaction between the -clusters, a strongly interacting Bose-gas with coherent properties may be formed [3]. A mixed phase of fermions and -particles is expected in N=Z nuclei below the threshold. It has been pointed out that this transition from the fermions fluid to Bose-gas is a second order phase transition [6]. We may observe that the study of -clustering has brought a large range of concepts into nuclear physics.

The present article is organized in the following way. A brief overview of the experimental results in cluster radioactivity, theoretical methods for interpreting the results, and extrapolation of the theory to the unknown super heavy region is given in the next section. It is followed by a discussion on the cold fission phenomenon. Cold heavy cluster formation in nuclear reactions and -clustering in light nuclei are discussed in the subsequent sections.

Cluster Radioactivity

General

Radioactive decay by emission of fragments heavier than -particle is a relatively recent observation and for this historical reason such decay is termed as cluster radioactivity. This convention leaves -radioactivity with its well established name although -particle is a good enough cluster. Many high Z nuclei decay through the emission of heavy particles, such as, ^{14}C, ^{24}Ne, ^{30}Mg, and ^{34}Si with $T_{1/2}$ in the range of few years to 10^{19} years. The first experimental identification for such a phenomenon was accomplished by Rose and Jones[1]. A rare class of events in the spontaneous fission where the fissioning nucleus undergo a cold rearrangement of the initial nucleus to the ground states of the fragments can also be considered as a manifestation of cluster radioactivity. A unified description of -decay, cluster radioactivity, and cold fission is highly desirable and many theoretical approaches have been proposed towards this goal.

Nuclear chart of experimentally determined cluster decay modes is given in Fig.1. There are two dozen nuclei from ^{221}Fr to ^{242}Cm emitting light nuclei from ^{14}C to ^{34}Si, correspondingly, leaving a daughter nucleus around ^{208}Pb. The type of cluster decay and the decimal logarithm of the half life in seconds for cluster and -decay are given for each parent nucleus. It may be noted that the -decay is a very dominant mode in these nuclei. Experimentally, one of the major problems was to suppress the enormous -particle background. In the first experiment performed by Rose and Jones [1], which ran six months in order to obtain 11 events of the cluster decay, a silicon E-E telescope directly viewing the source was used. The strong -particle background damaged the silicon detectors after irradiation with about 10^9 /cm^2 and the detectors were replaced as and when this limit was reached. In an experiment performed at Orsay [8], the unwanted -particles were deflected by a strong magnetic field produced in the superconducting spectrometer SOLENO and selected only ^{14}C to reach the detector in the focal plane. A source of about 300 times stronger than that used by Rose and Jones was employed so that number of days to obtain about a dozen events were reduced to five. With this high efficiency setup it was possible to discover [8] fine structure in cluster decay and to perform accurate experiments using high quality implanted sources [9]. There were also other spectrometer setups used for the discovery depicted in Fig.1. Solid state nuclear track detectors were also extensively used for investigations in this field (see for e.g. [10]) since they can record carbon and other heavy ions incidences while being insensitive to alpha and other low Z ions. They are made from polyethylene terephtalate or from a phosphate glass and are cheap and handy. But they do not deliver information online; only after suitable post-irradiation chemical etching the recorded ion tracks becomes visible under microscope for manual or computer aided counting.

Theoretical Models

Gross features of the cluster radioactivity places it in an intermediate position between the -decay and the spontaneous fission. There are two possible theoretical approaches for understanding the cluster decay, either as an adiabatic fission-like process or as a sudden two-step alpha-decay-like

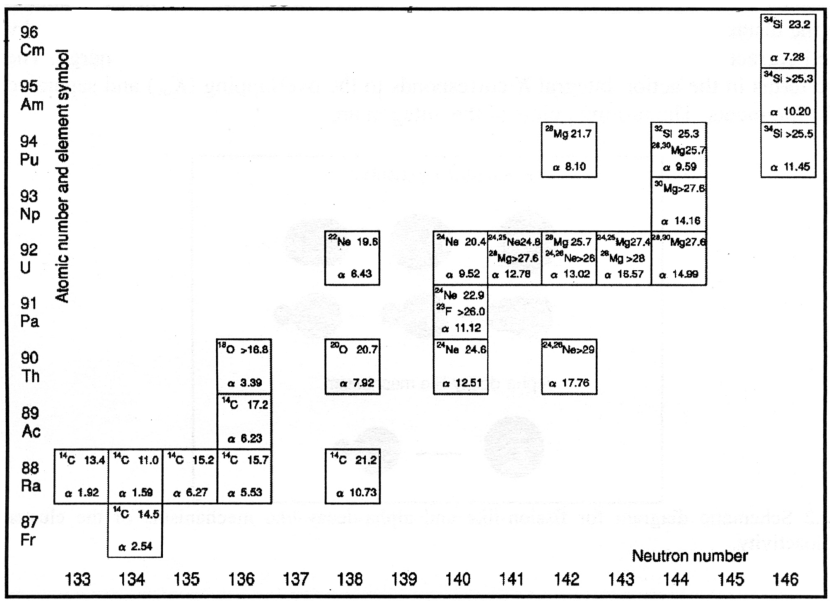

Fig. 1 Nuclear chart showing experimentally determined cluster decay modes and decimal logarithm of the cluster and -decay half-lives (from [7]).

process (see [11] for a topical review). The fission-like approach has evolved into a model called Super Asymmetric Fission (SAF) which treats cluster radioactivity as a dynamical mass fragmentation process. The alpha-decay-like approach treats cluster radioactivity as emission of heavy cluster through the Coulomb barrier, similar to Gamow's theory of -decay; including the theory of formation of the cluster in the nucleus. A visualization of fission-like and alpha-decay-like mechanisms of the cluster radioactivity is given in Fig. 2. Potentials relevant in these extreme pictures for the decay ^{222}Ra ^{208}Pb+^{14}C are given in Fig. 3. One can see a huge difference between the potentials used in the two approaches.

In the analytical super asymmetric fission(ASAF) model by Poenaru et. al [12] the half-life of a parent nucleus(A,Z) against spliting into a cluster (A_e,Z_e) and a daughter (A_d,Z_d) is calculated by using the Wentzel-Kramers-Brillouin (WKB) semiclassical approximation.

$$T = [(h \ln 2) / (2E_v)]\exp (K_{ov} + K_s),$$

$$K = K_{ov} + K_s = \frac{2}{\hbar} \int_{R_a}^{R_b} 2 \{[E(R) \quad E_{cor}] \quad Q\}^{1/2} dR$$

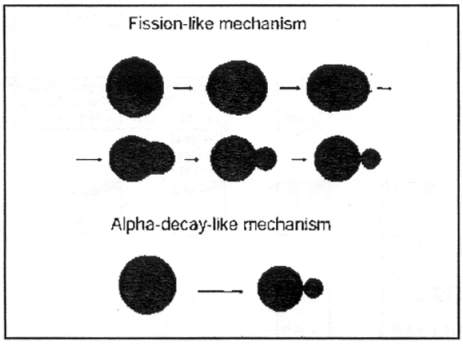

Fig. 2 Schematic diagram for fission-like and alpha-decay-like mechanisms of the cluster radioactivity.

where Q is the cluster decay energy (Q-value), =mA_eA_d/A is the reduced mass, m is the nucleon mass, and E(R) is the interaction energy of the two fragments separated by the distance R between centers, E_{cor} is a correction energy similar to the Strutinsky shell correction, h is the Plank constant and E_v is the zero point vibration energy. The two terms in the action integral K correspond to the overlapping (K_{ov}) and separated (K_s) fragments. The turning points of the integral are

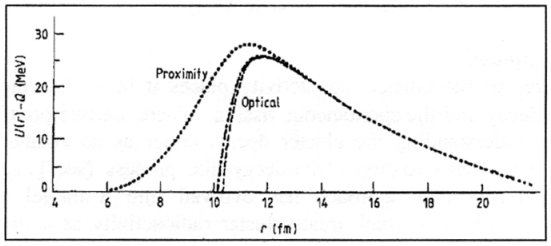

Fig. 3 *The barriers for the decay ^{222}Ra $^{208}Pb+^{14}C$ in the fission and alpha-decay like approaches. The fission-like approach was computed with the proximity potential and the alpha-decay-like approach was computed with the real part of two very different optical potential parameters.*

$$R_a = R_i + (R_t - R_i)\,[(E_v + E^*) / E_b^0 E\,]^{1/2},$$

$$R_b = R_t E_c \frac{\frac{1}{2} \quad \frac{1}{4} \quad (Q \quad E_v \quad E^*)E_l / E_c^2}{(Q \quad E_v \quad E^*)}^{1/2},$$

where E* is the excitation energy concentrated in the separation degree of freedom, $R_i=R_0-R_e$ is the initial separation distance, $R_t= R_e+R_d$ is the touching point separation distance, $R_j = r_0 A_j^{1/3}$ (j=0,e,d; r_0=1.2249 fm) are the radii of parent, emitted, and daughter nuclei, and $E_b^o = E_i$-Q is the barrier height before correction. The interaction energy at the barrier top, in presence of a non-negligible angular momentum l, is given by

$$E_i = E_c + E_l = (e^2 Z_e Z_d / R_t) + \ 1\,(l + 1) / (2 \quad R)$$

The alpha-decay like approach introduces a pre-formation probability of the cluster in the parent nucleus[11,13]. A quantum tunneling of the cluster through a barrier V(R) where the V(R) is determined as a sum of an attractive nuclear potential, a repulsive Coulomb potential and a centrifugal potential, is assumed. The potential V(R) is a function of only the radial coordinate R which is the separation between the mass center of the cluster and mass center of the daughter nucleus. Three classical turning points for the above potential denoted as R_1, R_2 and R_3 in order of increasing distance from the origin are obtained by numerical solutions of the equation V(R)=Q. The decay-width can be written as

$$P_c F_c \exp \quad 2 \int_{R_2}^{R_3} dR K(R)$$

where P_c is the pre-formation probability of the cluster in the parent nucleus, and F_c describes the motion of the cluster between the first and second classical turning points. The exponential factor is known as the Gamow factor where K(R) is the wave number given by

$$K(R) = \sqrt{(2 \quad / \hbar^2)|Q \quad V(R)|}$$

The cluster decay half life is given by

$$T_{1/2} = \hbar \ln 2 /$$

Q-values and Half-Lives

The Q value for the cluster radioactivity, which play a very important role in their decay probability estimation, is given in Fig.4 (left panels) for known cluster decays. The Q values are related to the mass difference between the parent nucleus(A,Z), the cluster(A_e, Z_e) and the daughter nucleus(A_d, Z_d). The cluster radioactivity is energetically allowed if and only if the released energy $Q=M(A,Z)-[M_e(A_e,Z_e)+M_d(A_d,Z_d)]$ is a positive quantity, (Q >0). The atomic masses M, M_e and M_d are obtained from experimental measurements. To inspect for the shell effects, the Q-values for different kinds of cluster decay modes versus the neutron number of the daughter nucleus(N_d) are plotted in Fig.4 (right panels) with points belonging to same Z_d joined with lines. In the Q-value variation with N_d, a maximum value at the magic number N_d=126 can be observed almost as a rule. The variation with Z_d for Z_d=80-82 is, as expected, increasing towards the magic value Z_d=82 with an exception for ^{23}F radioactivity(almost the same value for Z_d=80 and 81). As for the clusters themselves, they are certain neutron rich nuclei and their nucleonic structure has also an influence.

The other important ingredient influencing the decay half-lives is the cluster-daughter nuclear interaction potential. The decaying particle tunnels through this potential barrier. The fission-like and alpha-decay like models predicts completely different shapes for the inner part of the potential barrier(see Fig.3). Alpha-like barriers normally are much more narrower than the fission-like barrier and

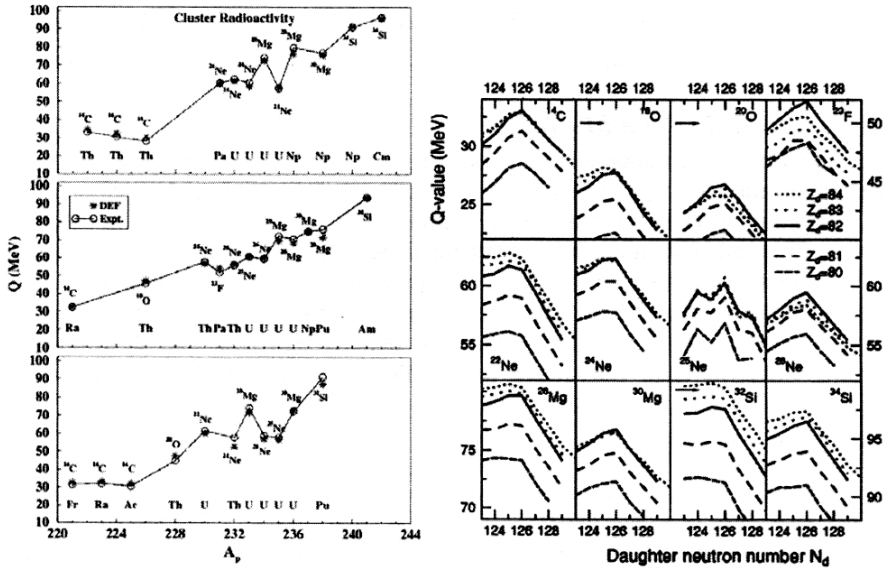

Fig. 4 (left panels) The Q-value as a function of parent nuclear mass number A_p. The experimental values(circles) are obtained from experimental masses while the DEF(asterix) is a model calculation [14]. (right panels) The Q-values for different kinds of cluster decay modes versus the neutron number N_d of the daughter nucleus(from [7]).

their increased penetrability is compensated by the small values of so called spectroscopic factors. The spectroscopic factor(S) represents the pre-formation factor P_c and it is obtained as a ratio of the calculated half-life to the experimental half-life. This peculiar compensation leads to a difficulty that the measured decay probabilities are reproduced by both the models. Therefore, getting independent information about the barriers, especially on their internal parts, has been seen as a priority [15] by investigators. A combined study of the cluster decay probability of a nucleus and fusion or elastic scattering of its decay products would provide new information on the mechanism of both the cluster radioactivity and the inverse process. To sum up the present status of calculations, a recent paper [16] brought out a list of cluster radio-activities together with experimental half-lives and corresponding spectroscopic factors as given in Table 1. The spectroscopic factors were seen to follow a simple rule as observed in earlier works [16].

Super Heavy Region

The cluster radioactivity is controlled by the Q-values and barriers and the role of Z=82, N=126

TABLE 1. Cluster decay modes, Q-values, decimal logarithm of experimental half-lives and spectroscopic factors.

Parent	Cluster	Q (MeV)	$\log_{10}T_{ex}$ (s)	S
^{212}Po	^{4}He	8.95	−6.52	1.88×10^{-2}
^{213}Po	^{4}He	7.833	−5.44	1.67×10^{-2}
^{214}Po	^{4}He	7.833	−3.78	3.45×10^{-2}
^{215}At	^{4}He	8.178	−4.00	1.31×10^{-2}
^{221}Fr	^{14}C	31.317	14.52	1.50×10^{-8}
^{221}Ra	^{14}C	32.396	13.39	1.55×10^{-8}
^{222}Ra	^{14}C	33.05	11.00	1.64×10^{-7}
^{223}Ra	^{14}C	31.829	15.20	2.85×10^{-9}
^{224}Ra	^{14}C	30.54	15.92	1.04×10^{-7}
^{225}Ac	^{14}C	30.477	17.34	8.14×10^{-8}
^{226}Ra	^{14}C	28.20	21.34	3.97×10^{-8}
^{228}Th	^{20}O	44.72	20.72	8.37×10^{-11}
^{230}U	^{22}Ne	61.40	19.57	6.72×10^{-12}
^{230}Th	^{24}Ne	57.571	24.64	1.87×10^{-13}
^{231}Pa	^{24}Ne	60.417	23.38	3.13×10^{-15}
^{232}U	^{24}Ne	62.31	20.40	9.77×10^{-14}
^{233}U	^{24}Ne	60.486	24.82	1.47×10^{-15}
^{234}U	^{24}Ne	58.826	25.25	1.54×10^{-13}
^{233}U	^{25}Ne	60.776	24.82	4.02×10^{-16}
^{234}U	^{26}Ne	59.466	25.07	1.67×10^{-14}
^{234}U	^{28}Mg	74.11	25.74	6.30×10^{-17}
^{236}Pu	^{28}Mg	79.67	21.67	2.83×10^{-17}
^{238}Pu	^{28}Mg	75.912	25.70	1.21×10^{-16}
^{238}Pu	^{32}Si	91.19	25.28	2.34×10^{-18}
^{238}Pu	^{30}Mg	91.19	25.28	2.34×10^{-18}
^{242}Cm	^{34}Si	96.509	23.15	1.10×10^{-19}

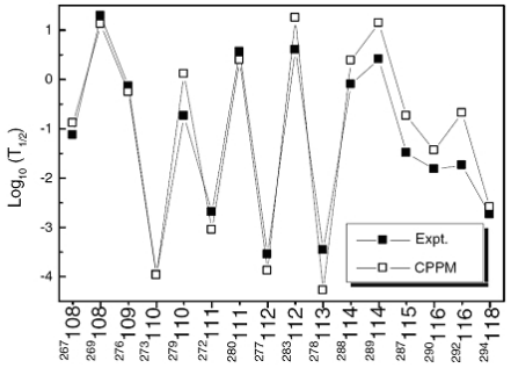

Fig. 5 Experimental and calculated (CPPM) decimal logarithm of alpha decay half lives for parent nuclei of Z=108-118 (from [18]).

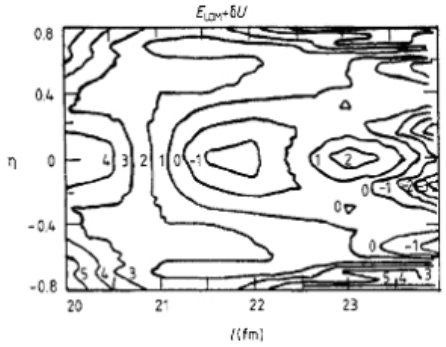

Fig. 6 Potential energy surface for ^{252}No nucleus as a function of elongation l and mass asymmetry parameter (from [11]).

(^{208}Pb) shell is evident in the experimentally observed cases. One of the fundamental factors in the study of super heavy elements is production and characterisation of doubly magic nucleus beyond ^{208}Pb region, where proton number Z=114, 120, 126 and neutron number N=172, 184 have been predicted to be magic numbers. Since it is difficult to obtain cluster decay data systematics for super heavy mass region, well tested models of cluster decay should be used for predictions in unknown regions. Compared to normal nuclei, magicity in super heavy nuclei are expected to be fragile since the region of enhanced shell effects are generally broad. Also, the quantum shell energy may favor shape deformations, i.e., special stability is achieved for deformed super heavy nuclei. These aspects make cluster decay calculations in super heavy mass region very challenging. A quantitative microscopic description is expected only by application of the nuclear density functional theory currently under development. Despite current limitations, there are several calculations available for the spontaneous fission and alpha decay processes. For example, experimental and calculated alpha decay half-lives of parent nuclei with Z=108-118 are shown in Fig.5 where calculations were done using the Coulomb and proximity potential model [17,18].

Cold fission

Introduction of shell effects in the potential energy surface (PES) for fission leads to multiple fission valleys in heavy nuclei, resulting in their multi-modal fission. For example, in the PES for ^{252}No in length l and in mass asymmetry co-ordinate (minimized relative to the deformation of each fragment ($_1$, $_2$) and the neck parameter ; =$(A_1-A_2)/(A_1+A_2)$, $A_1$and A_2 are fragment mass numbers), it can be seen that the two shell model valleys appear mainly due to the doubly magic structure of ^{132}Sn and ^{208}Pb(Fig.6) [11]. The first valley is with strongly elongated fragments and the second one is with nearly spherical fragments. The strongly elongated fragments in the valley lead to very excited fragments at scission. The spherical fragments in the valley lead to non-excited fragments in a cold fragmentation process known as cold fission. Such a rearrangement of large number of nucleons without excitation of the fragments is made possible by introducing the neck degree of freedom. In the framework of the two centre shell model, it is hard to imagine that the fragments remain non-excited in such a rearrangement. The distance between the fragments at the scission configuration for spherical fragments (cold fission) is much smaller than that for the normal fission. The released fission Q-value appear mostly as total fragment kinetic energy (TKE) for the cold fission. Extensive experimental and theoretical works were carried out to confirm the multi-model nature of the fission process. It is generally understood that the true cold-fission events have a low probability of occurrence (typically one out of 10^6 fission events). Evidently, new experiments are needed, in which the -rays and neutrons from each fragment are registered. In this way the cold fragmentation in

fission could be separated from the normal hot fission. Also characteristics of each valley could be experimentally determined and compared with the theoretical predictions. The study of tri-modal fission of ^{264}Fm is instructive[11]. The PES for ^{264}Fm is minimized at symmetric fragmentation (charge and mass asymmetries equal to zero). Close to the scission, three valleys could be observed for the symmetric fragmentation; one valley corresponds to a new type of fission with nearly spherical fragments, the second valley with one fragment spherical and the other very elongated and the third one with both fragments strongly elongated. From the point of view of mass distributions, the new nearly spherical fragments mode will be very similar to spontaneous fission. But the observed TKE distribution had two components. The component with high TKE is termed as Sn-radioactivity, since in this case the spherical Sn-fragments are emitted with almost no excitation energy. The compactness of the scission configurations together with absence of fragment excitation will lead to value of kinetic energy of the fragments much higher compared to spontaneous fission process, that almost approaching the Q-value.

Heavy Cluster Formation in Nuclear Reactions

In collision of two massive nuclei, competition between reaction channels is strongly dependent on the contact configuration of the interacting nuclei. The properties of the entrance channel, such as mass asymmetry, energy, angular momentum and deformations have a dominant role. Moreover, the potential energy surface which is engaged in evolution of the intermediate nuclear system is strongly modulated by the shell effects. The existence of minima caused by shell effects in the potential energy is likely to be responsible for manifestation of clustering phenomena in different reaction channels. In case of the cold fission (an exit channel phenomenon) the nuclear shells with Z=50 and N=82 were found to play an important role. In the case of the entrance channel phenomenon, the nuclear shells with Z=28, 82 and N=50, 126 would be determining factors. Mass and energy distributions in quasi-fission were studied recently [19] for presence of clustering due to shells. It was found that clustering phenomena have a great influence on the formation of the reaction products for fusion-fission and quasi-fission processes.

Signatures for possible cluster emission from compound nuclear excited states were discussed in [20]. For example, in the decay of ^{212}Po* by -emission, the daughter will be doubly closed ^{208}Pb*, which may give away all its excitation energy as kinetic energy of -particle and recoiling daughter due to strong shell guided clustering effects, thereby enhancing the average kinetic energy of the -particles. This hypothesis was examined in [21] for the decay of ^{208}Po* populated in a heavy ion reaction. Within the experimental uncertainties no evidence for excess kinetic energy was found.

Alpha Clustering in Light Nuclei

As mentioned in the Introduction, the theory of alpha clustering in light nuclei has reached a much sophisticated level and its success with experiments shows that alpha particle behaves as a constituent unit in the relevant nuclear states. In understanding of general nuclear clustering phenomena, these theoretical methodologies will be useful and, therefore, it is important to have survey of relevant literature giving theoretical and experimental results. There are several studies concentrating on ^{8}Be, ^{12}C, ^{16}O, ^{20}Ne and such -nuclei, (for a recent conference proceeding on this topic, see[22]) however, here, discussion is limited to some recent works on ^{12}C to highlight the nature of present studies.

Recently, -particle Bose-Einstein condensation in light nuclei, especially in ^{12}C and ^{16}O was proposed[3]. In early days, the second excited state of ^{12}C (7.65 MeV 0^{+}), the famous Hoyel state, was assigned a linear 3- structure by Morinaga[23]. Later, it was shown that this state which is 0.39 MeV above the 3- threshold, has a well developed -cluster structure with a ^{8}Be- configuration. In 2001, Tohsaki et al. [3] conjectured that this may be a BEC state of -particles in that weakly interacting three -particles are sitting in the lowest single particle 0s state like a gas with dilute density distribution obeying Bose statistics. The rms radius calculated for this BEC state is 4.29 fm far greater than the experimental rms radius of the

ground state, 2.65 fm. The dilute property of this state had not been confirmed in a direct way till the analysis of Ohkubo and Hirabayashi[4]. In [4], the authors confirmed the dilute nature from the Airy structure observed in the experimental +12C rainbow scattering data[24,25]. The experimentally observed rms radius of the BEC (Hoyel) state was 4.31 fm, which is in agreement with the theoretical value.

From the time of publication of [23], there have been unsuccessful searches for a 2^+ state in ^{12}C that is first member of a rotational band with the Hoyel state as the band-head. Recently many new experiments have been performed probing the triple alpha continuum of ^{12}C. A 2^+ sate has been suggested in two different $^{12}C(\ ,\ ')^{12}C^*$ experiments [24,26] but at two different energies, making the question unsettled. A recent experiment [27] using the $^{12}C(^{12}C,3\ )$ reaction presented evidence for a state consistent with [24]. Another discussion is around the broad 10.3 MeV state in ^{12}C that was thought to be the 2^+ member in the rotational band for many years. Scattering experiments provided evidence that it is a 0^+ state, and precise angular distributions confirming the 0^+ multi-polarity of this state was obtained in [24]. The exact energy of this state, which has got an astrophysical significance as discussed in [28], is still not clear from the different experiments, and efforts are continuing for determining its energy.

Summary

A quarter century long study of the cluster radioactivity has established a firm knowledge base for the phenomenon. It emerges that the cluster emission is not an isolated phenomenon, but has many commonalities with the -decay and spontaneous fission. -clustering in light nuclei and heavy cold cluster formation in quasi-fission reactions has also enriched this active field of research. It is recognized that shell closure in one or both fragments involved is responsible for the cold nature of the process.

References

1. H. J. Rose et al. Nature 307, 245 (1984).
2. A. Sandulescu, D.N.Poenaru and W.Greiner, Sov. J. Part. Nucl. 11, 528 (1980).
3. A. Tohsaki et al., Phys. Rev. Lett. 87, 192501(2001)
4. S.Ohkubo and Y. Hirabayashi, Phys. Rev. C 70, 041602(R)(2004).
5. K. Ikeda, H.Horiuchi and S.Saito, Prog. Theor. Phys. , Supplement, 68, 1 (1980).
6. P. Schuck et al. Nucl.Phys. A 738 (2006) 94. W. von Oertzen, EPJ. A 29 133(2006).
7. D.N.Poenaru, Y.Nagame, R.A.Gherghescu and W.Greiner, Phys. Rev. C 65, 054308(2002).
8. L. Brillard, A.G. Elayi, E.Hourany, M.Hussonnois, J.F.Le Du, L.H.Rosier and L. Stab, C.R.Acad.Sci. Paris 309, 1105(1989)
9. E. Hourany et al. Phys. Rev. C 52, 267(1995)
10. P.B.Price, Annu. Rev. Nucl. Part. Sci., 39, 19(1989)
11. A. Sandulescu, J. Phys. G: Nucl. Part. Phys. 15, 529 (1989)
12. D.N.Poenaru, W.Greiner and R.Gherghescu, Phys. Rev. C 47, 2030(1993)
13. Z.Ren, C.Xu and Z.Wang, Phys. Rev. C 70, 034304(2004)
14. A.Bhagwat and Y.K.Gambhir, Phys. Rev. C 71, 017301(2005)
15. A.A.Ogloblin, S.P.Tretyakova, R.N.Sagaidak, S.A.Goncharov and G.A.Pik-Pichak, Nucl. Phys. A738, 313(2004).
16. M. Bhattacharya and G.Gangopadhyay, Phys. Rev. C 77, 027603(2008)
17. K.P.Santhosh, R.K.Biju and and Antony Joseph, J. Phys. G: Nucl. Part. Phys. 35 085102 (2008).
18. K.P.Santhosh and R.K.Biju, J. Phys. G: Nucl. Part. Phys. 36, 015107(2009).
19. M.G.Itkis, G.N.Knyazheva and E.M.Kozulin, Int. Jour. Mod. Phys. E, 17, 2208(2008)
20. P.Armbruster, Rep. Prog. Phys. 62, 465(1999).
21. Bency John, R.K.Choudhury, B.K.Nayak, A.Saxena, and D.C.Biswas, Phys. Rev. C 63, 054301(2001)

22. International Journal of Modern Physics E, Vol 17, No.10(2008)

23. H. Morinaga, Phys. Lett. 21, 78(1966)78

24. Bency John, Y.Tokimoto, Y. –W. Lui, H.L.Clark, X.Chen, and D.H.Youngblood, Phys. Rev. C 68, 014305(2003).

25. A. Kiss et al., J. Phys. G 13, 1067(1987); S.M.Smith et al., Nucl. Phys. A207, 273(1973); B.Tatischeff and I, Brissaud, Nucl. Phys. A155, 89(1970).

26. M.Itoh et al., Nucl. Phys. A738 (2004)268.

27. M.Freer et al., Phys. Rev. C 76, 34320 (2007)

28. H.O.U.Fynbo at al., Nature 433,136 (2005).

One and Two Proton Radioactivity

Dr. Asok Goswami *passed M.Sc (Chemistry) from Burdwan University and joined BARC Training school in 1979. After passing training school, he joined Radiochemistry Division, BARC. He obtained his Ph.D. from Mumbai University in 1992. His areas of research include nuclear fission, nuclear reactions, prompt gamma neutron activation analysis, non destructive assay techniques, and diffusion of ions through ion exchange membranes. He has more than 80 publications in international journals.*

A nucleus undergoes radioactive decay due to its inherent thermodynamic instability. The study of the classical decay modes of nucleus viz. alpha decay, beta decay, gamma decay and spontaneous fission decay has helped in understanding the cause of nuclear instability in terms of composition (neutron and proton number) and structure (internal arrangements of nucleons in definite energy levels) of the nucleus. Thanks to the development of sophisticated experimental techniques for detecting very rare events, newer decay modes have been discovered since 1980. The unstable nuclei exhibiting these decay modes can be classified as: (i) one proton (1p) emitters (about 25) (ii) two proton (2p) emitters (3) and (iii) exotic cluster emitters (C, O, F, Ne, Mg, Si)(about 25). Well known phenomenon like - delayed n or p emission occurs from the excited state of a nucleus, and is not considered as the radioactive decay modes. The subject of the present article is: one(1p) and two proton (2p) radioactivity. The subject has been extensively reviewed in reference 1 and 2.

Fundamentals of one- and two- proton Radioactivity

The 1p radioactivity can be represented as:

$$A \quad B + p$$

where the nucleus A decays by a proton emission to the nucleus B. The necessary condition for a nuclide to undergo any type of radioactive decay is that the mass of the nuclide should exceed the sum of the masses of all the decay products so that the Q- value for the process is positive. For example, for 1p radioactivity, the condition can be expressed as:

$$Q_p = (M_{Z+1}) - M_Z - m_p - m_e)c^2 > 0$$

$M_{Z+1,}$ and M_Z are the atomic masses of the parent (A) and daughter (B) nuclides, and m_p and m_e are the masses of proton and electron respectively, and C is the velocity of light. In terms of binding energy, the Q_p can be written as:

$$Q_p = (B_Z - B_{Z+1})$$

$$B_Z = (ZM_H + Nm_n - M_Z)\, C^2$$

Similarly, for 2p radioactivity the necessary condition is:

$$Q_p = (B_Z - B_{Z+2}) > 0$$

Why one and two proton radioactivity are so rare that it took nearly a century after the discovery of radioactivity by Becquerel (1996) to conclusively prove the existence of these decay modes? The liquid drop model of nucleus gives a straightforward answer to this question. According to this model, a nucleus behaves like an incompressible charged droplet of a liquid. The stability of the droplet is governed by attractive nuclear interactions between the constituent (n and p) of the nucleus and the counterbalancing force of surface tension (arises due to finite size of the drop), Coulomb repulsion between the protons, and by an asymmetry term that arises due to the difference in neutron and proton numbers in a nucleus. There is an additional term due to pairing effect which makes even- Z even -N nucleus more stable compared to even-Z odd-N, odd- Z even- N and odd- Z odd –N nuclei. In order to form a stable nucleus, a certain equilibrium number of protons and neutrons are needed. Thus a plot of neutron versus proton number for the known stable isotopes (259) gives a beta stability line along which nuclides are stable. Upto mass number 40,

Dr. A. Goswami, Radiochemistry Division, Bhabha Atomic Research Centre, Mumbai 400 085;
E-mail: agoswami@barc.gov.in

TABLE 1. 1p radioactive nuclides and their proton-decay energies, half-lives, partial half-lives and branching ratios.

Isotope	E_p/keV	$T_{1/2(exp)}$	$T_{1/2(p)}$	$T_{1/2(\ )}$	B_p(%)	B (%)
^{53m}Co	1560	247±12 ms	17 sec	200 ms	1.5	98.5
^{105}Sb	478		50 sec	500 ms	1	99
^{109}I	813	103±5 s	103±5 s	250 ms	99.84	0.04
^{112}Cs	807	500±100 s	500±100 s	100 ms	99.6	0.5
^{113}Cs	959	28±7 s	28±7 s	200 ms	99.99	0.01
^{146}Tm	1198	72±23 ms	95 ms	300 ms	76	24
^{147}Tm	1051	560±40 ms		300 ms	21	79
^{150}Lu	1263	35±10 ms	46±10 ms	150 ms	77	23
^{151}Lu	1233	85±10 ms		250 ms	70	30
^{156}Ta	1022			1.0 sec	84	16
^{160}Re	1261	790±160 s	1.31±0.16 ms	600 ms	60.4	0.1

these stable nuclides are characterized by an approximately equal number of protons and neutrons. Beyond this mass number, more neutrons per proton are required to overcome the Coulomb repulsion of protons to form a stable atomic nucleus. (N-Z)=44 for the heaviest stable nucleus ^{208}Pb. If extra neutrons or protons are added to a stable nucleus, the (n-p) equilibrium is disturbed and the resulting nucleus decays by emission of $^{-}$ or $^{+}$ particle (transformation of a neutron to proton or vice versa) to attain stability. Why proton rich nuclei, instead of decaying by proton emission, tend to decay by emission of $^{+}$ particle? The reason is that, near the beta stability line, the protons are bound to the nucleus by nuclear force and extra energy has to be supplied to such a nucleus (in the form of excitation energy by way of some nuclear reaction) to take the proton off the nucleus. In other words, the Q- value for 1p/2p radioactivity for the proton rich nucleus near the stability line is always negative while that for $^{+}$ decay is positive. Hence no proton radioactivity is possible from the ground state of a nucleus near the stability line. However, if we keep on adding extra protons to a nucleus, the binding energy of the successive proton decreases and a point is reached when the last proton's binding energy becomes zero. Such proton excess nuclides fall on a line called proton drip line along which the binding energy of the last proton is zero. Further addition of protons to such nuclide would make them unstable to decay by proton emission. Thus, to observe one or two proton radioactivity, one has to prepare nuclides beyond the proton drip line by way of nuclear reactions. The task is not easy as experimental hurdles are too many. The production rates for such neutron deficient nuclides are extremely low, half-lives are short, and energies of emitted protons are relatively small. Hence, one and two proton radioactivity remain rare decay modes till today. About 25 nuclides have been identified that decay by proton emission and only 3 nuclides have been identified that decay by 2p emission from ground state. A representative list of 1p and 2p radioactive nuclei are given in the Table 1 and 2 respectively.

As seen from the tables, half-lives for 1p and 2p emitters are in the range of s to ms and major competitor to proton decay is $^{+}$ decay. In Table 1, where the sum of branching ratios is not ~100%, the remaining part goes to alpha decay. Also it is seen that 1p emitters are mostly concentrated in the mass

TABLE 2. 2p radioactive nuclides and their proton-decay energies, half-lives, partial half-lives and branching ratios.

Isotope	2p decay-energy (MeV)	Branching Ratio (I_{2p}/I_{+})	Partial Half-life(ms)
^{45}Fe	1.151±0.015	0.65±0.05	$3.9\ ^{0.4}_{0.4}$
^{48}Ni	1.35±0.02	$2.1\ ^{2.1}_{0.7}$	$8.4\ ^{12.8}_{7.0}$
^{54}Zn	1.48±0.02	$3.2\ ^{1.8}_{0.8}$	$3.7\ ^{2.2}_{1.0}$

region 100-115 (Z~50) and 140-160 (N~82) indicating that nuclear structure can influence the decay properties of such nuclides.

Figure 1 shows the binding energy of neutron deficient N=80 isotones calculated using the mass formula of MÖller and Nix [3]. The isotonic binding energy parabolas connect the odd even and even-even isotones, respectively. The distance between the two parabolas give the proton pairing energy $_p$. The binding energy of isotones exhibit maximum values, and the change of the slope allows for the positive Q_p values near the maxima. Thus the first proton unbound isotone is ^{149}Tm(Z=69) as seen from the figure. The Q_p for the decay ^{151}Lu ^{150}Yb + p is large enough (1.24MeV) to have a measurable proton decay branch as seen from the table 1. It is to be noted from the table 1 and 2 that all p emitters are odd Z isotopes while all 2p emitters are even Z isotopes. This can be understood from Fig. 2. The sequential emission of two protons is possible if the mass of the one-proton daughter nucleus is smaller than the mass of the two-proton emitter but larger than the mass of the two-proton daughter (left). If the intermediate state is higher in mass than the initial state, one-proton emission is energetically forbidden, and the decay occurs directly to the two-proton daughter (right). Proton pairing energy plays a pivotal role in this. Due to the gain of stability, the mass of the even-Z 2p emitter is smaller than the mass of the intermediate odd-Z 1p emitter, and therefore 1p emission cannot occur.

Hence 2p emission becomes the favoured mode of decay for such nuclei. This condition is fulfilled for medium-mass proton-rich nuclei around

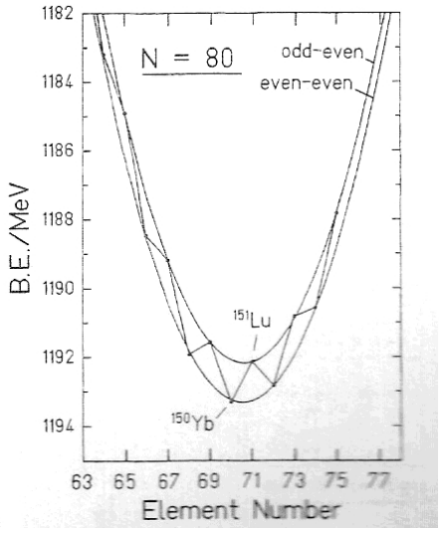

Fig. 1 Binding energies of neutron deficient N=80 isotones [1].

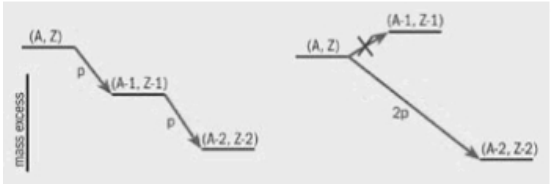

Fig. 2 Schematic energy level diagram showing sequential emission of two proton and direct emission of two proton [4].

A=40-50 and as seen from Table 2, known 2p emitters fall in this mass region.

The next thing to understand is the mechanism of 1p and 2p decay. As such it is the same as that of -decay. Even if a proton is unbound to a nucleus, it

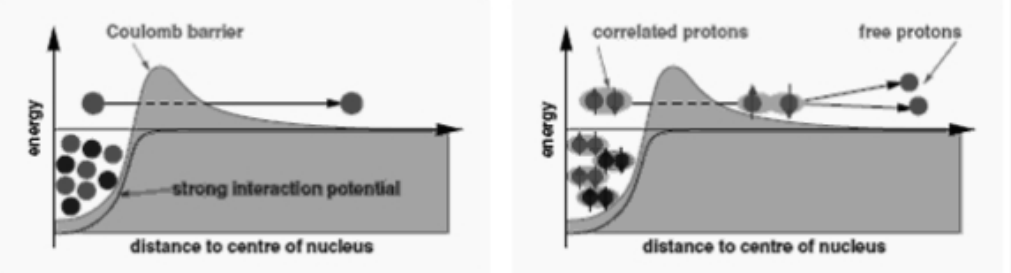

Fig. 3 Schematic representation of tunneling through the Coulomb barrier for decay by 1p and 2p emission. For one-proton emission (left), the tunneling depends mainly on the barrier height. For two-proton emission (right) the correlation between the two protons may influence the tunneling process [2].

has to cross a finite Coulomb barrier to come out of the nucleus. Thus the decay is not instantaneous. There is a finite half-life for the decay. It is worthwhile to mention that the particle is unbound to ^{238}U nucleus (Q >0), yet ^{238}U decays with half-life more than billions of years due to the existence of high Coulomb barrier for the decay. Figure 3 shows the tunneling process involved in the 1p and 2p emission.

However unlike -decay, observation limit for 1p and 2p radioactivity exists due to the severe experimental limitations. Thus, with present day experimental set-up, it is not possible to measure half life less than about 1 s for proton decay. On the other hand, proton decay faces severe competition from $^{+}$ decay, so the barrier penetration half-life should be comparable or shorter than the $^{+}$ decay half-life so that the proton decay branching ratio is significant (see table 1 & 2). This sets upper limit of the half-life to about 1 ms. Thus the chance of observing proton decay with the partial half-life of even a few seconds is remote. Figure 4 shows the calculated barrier penetration half-lives for a proton as a function of the nuclear charge and decay energy.

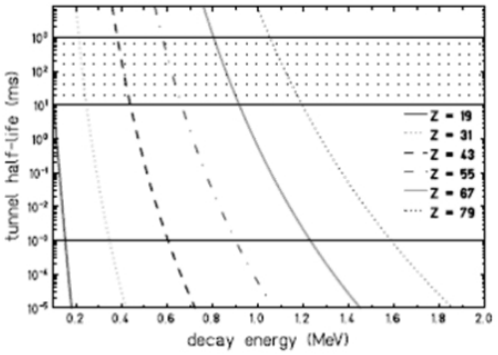

Fig. 4 Barrier-penetration half-lives for a proton as a function of the nuclear charge and the decay energy. The half-lives are calculated from Coulomb wave functions using the Wigner single-particle width. The horizontal line gives the lower detection time limit, whereas the hatched area gives typical -decay half-lives [2].

Experimental Techniques

Two different approaches have been used to produce short lived neutron deficient isotopes near the proton drip line: (1) Spallation reactions with high energy proton beams [5] and (2) heavy ion fusion reactions of neutron deficient projectile and target nuclei [6,7]. For example, ^{96}Ru target (97.9% enrichment) was irradiated with 261 MeV ^{58}Ni projectiles at GSI to produce a proton emitter ^{151}Lu for the first time in 1980 [8].

As stated earlier, production rates for proton emitters are extremely low, the half-lives are extremely short, and proton energies are relatively small. Hence, a pre-selection of the desired proton emitters from a host of the other undesirable reaction products, and the incident beam is necessary before their decay properties can be studied. The GSI separator for heavy ion reaction products (SHIP) [9] has been used successfully to discover ^{151}Lu and other proton emitters. Here recoiling reaction products from the target are separated based on momentum and ionic charges and are implanted on a Si detector system for detection of proton decay. The separation time for the system is about 0.5-2 s,

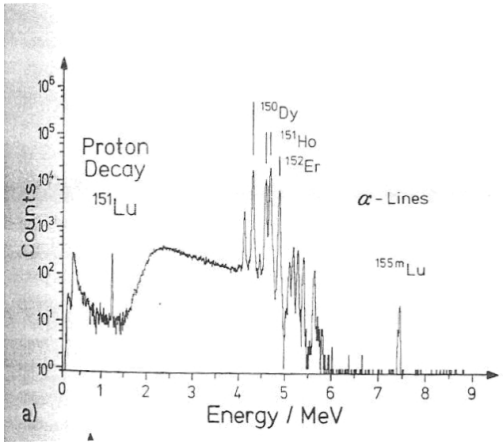

Fig. 5 Energy spectrum showing the ^{151}Lu proton decay line at 1.23 MeV during the irradiation of a ^{96}Ru target with 261-MeV ^{58}Ni projectiles at SHIP[12]. -decay lines of other reaction products are at distinctly higher energy.

setting lower limit of detection of proton emitter half-lives. The suppression factor of the primary beam is high (10^8-10^{16}), allowing rare events to be observed. Similarly Fragment Mass analyser (FMA) at the ATLAS accelerator in Argonne National Laboratory, which is recoil mass separator, has been used successfully to discover the heaviest proton emitter (^{185}Bi) known so far.

The discovery of ground state 2p radioactivity of ^{45}Fe was reported in the year 2002. The experiments were performed at the SISSI/LISE3 facility of GANIL [10], France and FRS of GSI, Germany [11]. ^{45}Fe was produced by fragmentation of a primary ^{58}Ni beam. The detection set up for two proton radioactivity is rather elaborate. For example, at GSI, a Si telescope of seven elements , surrounded by a high efficiency NaI array, was used. The 2p radioactivity was confirmed by a series of elimination processes of the competitive decay modes: (1) $^{+}$ decay followed by proton emission was eliminated by non observation of two 511 keV gamma ray in coincidence with the proton, (2) Smaller width of the 2p emission (ground state emission) compared with the $^{+}$ delayed p emission, and (3) Confirmation from daughter half-life.

Results

Figure 5 shows the energy spectrum of the decay products from the heavy reaction residues produced by irradiation of ^{96}Ru target with 261 MeV ^{58}Ni projectiles. The residues were separated by SHIP. About 100 decay events due to 1p decay of ^{151}Lu at 1.23MeV were recorded. The proton decay energy was well separated from the -lines of other reaction products. Figure 6 shows the 2p decay energy spectrum of ^{45}Fe from the GANIL experiment (left) [10] exhibiting a peak at 1.14 MeV, and GSI experiment (right) [11] showing a peak at 1.1 MeV. It is to be noted that both the experiments observed the total energy released in the decay, neither the individual proton energies nor their relative emission angles. The events seen at high energy are not due to 2p emission. As can be seen from the figures, only a few events were recorded in both the cases, showing the sensitivity achieved in the experiments.

From the point of nuclear spectroscopic aspects and predictions of 1p radioactivity, nuclides have been classified into several regions. Some of them are: (1) Neutron deficient Z<50 region where the proton drip line is relatively close to the valley of beta stability. This region is of interest for understanding the astrophysical rapid-proton-capture (rp) process. Figure 7 shows the proton drip line in the region Cu-Zn that has been identified, and a possible path of the rp process. Likely proton emitters are also indicated in the figure. (2) The transitional region near Sn where proton emitters like ^{105}Sb, ^{109}I, ^{112,113}Cs, ^{146,147}Tm have been identified. Calculations of half-lives, possible shell-model states and the ground state deformations have been resonably successful in this region. (3) Neutron deficient heavy nuclei (Z>76), which have high probability of alpha decay. Proton radioactivity of ^{165,166,167}Ir, ^{171}Au and ^{185}Bi have been reported [10]. Interesting information regarding validity of the existing models of nucleus is being obtained from the study of such nucleus. Efforts are on for identification of new 1p and 2p emitters. New facilities giving radioactive ion-beams are coming up which will facilitate further research in this area. The mechanism of 2p emission is still not clear. Study on the correlation of the protons emitted can throw light on the process. The two-proton decay

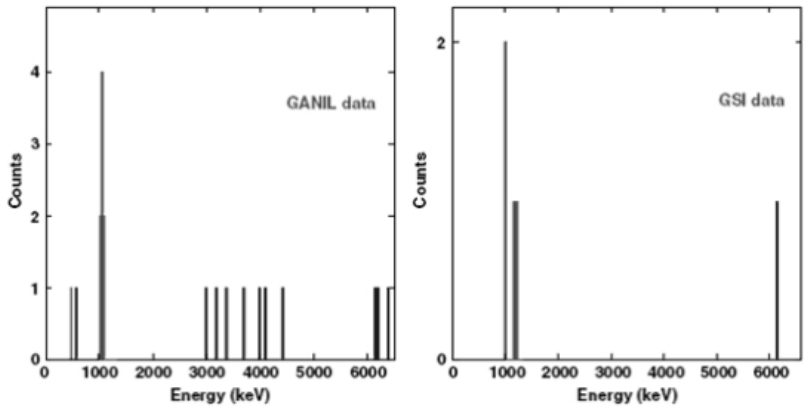

Fig. 6 (Left) ^{45}Fe decay-energy spectrum from the GANIL experiment exhibiting a peak at (1.14 ± 0.04) MeV [10]. (Right) ^{45}Fe decay-energy spectrum from the GSI experiment showing four events at 1.1(1) MeV [11]. Both spectra also show events at higher energies.

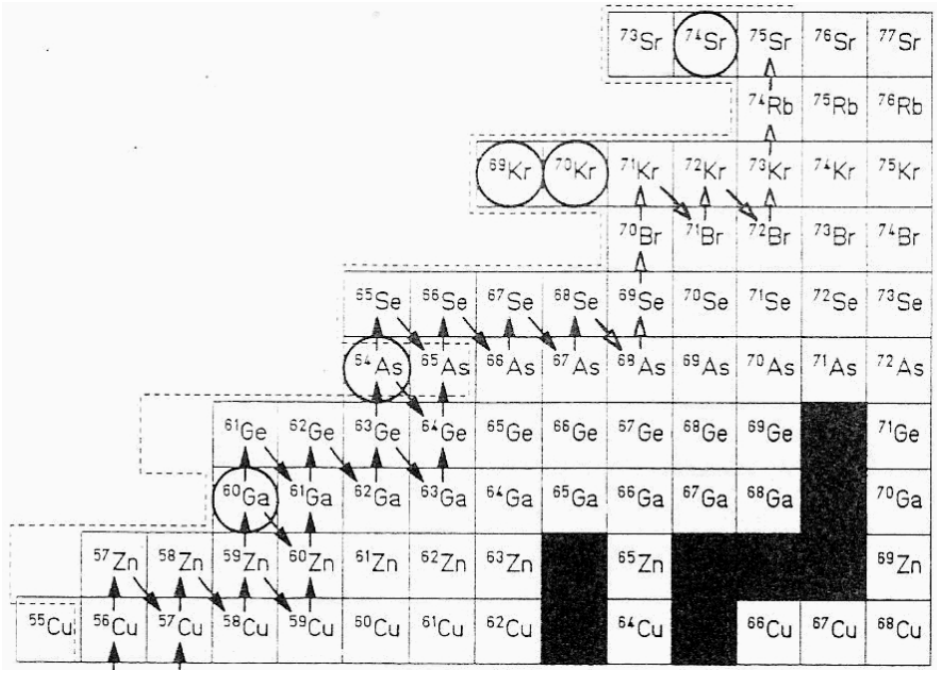

Fig. 7 Section of the chart of nuclides in the region of interest for the astrophysical rp process. The nuclei marked by circles have been identified at GANIL. The nuclei to the left of the dashed line are predicted to be 1p emitters. The arrow indicates a possible route for the rp process [13].

may open an original route towards studying pairing in the atomic nucleus. In addition, this research will allow determination of masses for nuclei beyond the limits of stability via the measurement of the Q value, which then allows mass-model predictions far away from the stability line to be tested. By comparing experimental results and theoretical calculations, the single-particle structure of extremely proton-rich nuclei might become accessible. A deeper understanding of nuclear

structure can only be obtained by studying nuclei far away from stability [4].

References

1. S. Hofmann: Radiochimica Acta, 70/71, 93 (1995)
2. Bertram blank and Marek Ploszajczak: Rep. Prog. Phys. 71, 046301 (2008).
3. P. MÖller and J.R. Nix: At. Data and Nucl. Data Tables 26, 165 91981).
4. Cern Courier Dec.1, 2002.
5. J.M. D'Auria et al. :Nucl. Phys. A301, 397 (1978).
6. C. Bruske et al. : Nucl. Instrum. Methods 186, 61 (1981).
7. J.M. Nitschke et al. : Nucl. Instrum. Methods 206, 341 (1983).
8. S. Hofmann et al. in Proc. 4th Int. Conf. on Nuclei Far from Stability. CERN 81-09, Geneva, 190 (1981).
9. G. Munzenberg et al. : Nucl. Instrum. Methods 161, 65 (1979).
10. J. Giovinazzo et al. : Phys. Rev. Lett. 89, 102501 (2002).
11. M. PfÜtzner et al. : Eur. Phys. J. A14, 279 (2002).
12. S. Hofmann et al. Z. : Phys. A305, 111 (1982).
13. B. Blank et al. :Phys. Rev. Lett. 74, 4611 (1995)

Double Beta Decay – An Introduction

Dr. Vivek Datar *is senior scientist at Nuclear Physics Division, BARC. He obtained his B.Sc.(Hons) degree in Physics from Bangalore University in 1974 and Ph.D. from University of Mumbai in 1983. He did post-doctoral assignments at Institut de Physique Nucleaire (CNRS), Orsay France (1986-1987) and at the University of New York, Stony Brook, USA (1987-1988). His areas of work include low energy nuclear physics in general and, tests of conservation laws and symmetries, search for massive neutrinos, first evidence for -decay of 4^+ state in ^{8}Be and astrophysical $S_{17}(0)$ from ^{2}H(^{7}Be,^{8}B)n reaction at low energy using the ^{7}Be radioactive ion beam at the Nuclear Science Centre (now IUAC), New Delhi. He also helped set up a 1 m^2 plastic detector array for fast neutron spectral measurements using the time-of-flight technique. He received the N. S. Satyamurthy Award of Indian Physics Association 1989. He is a member of the Programme Management Committee of the India based Neutrino Observatory (INO), a collaborative project which aims to set up a large underground laboratory primarily for neutrino physics but which could also house other experiments that could benefit from being deep underground. He is also the Dean-Academic, Physical and Mathematical Sciences, BARC-HBNI and is an Adjunct Professor in the School of Natural Sciences, TIFR*

Introduction

Beta decay is a process where a neutron (proton) in a nucleus transforms to a proton (neutron) with the simultaneous emission of an electron (positron) and an anti-neutrino (neutrino) of the electron type. The decay, for example, can be written as

$$n \quad p + e + \bar{\nu}_e$$

or, when the neutron is bound in a nucleus,

$$_ZA \quad _{Z+1}A + e + \bar{\nu}_e$$

This process can also take place, if allowed by energy considerations viz. Q-value > 0, for a bound proton but is energetically disallowed for a free proton. In a related process, termed electron capture, an inner shell electron reacts with a proton in a nucleus producing a neutron and a mono-energetic neutrino. The first step in understanding beta decay was taken by Pauli [1], with his suggestion of a neutral, light, weakly-interacting spin half particle emitted along with beta particles. This hypothesis explained the continuous energy spectrum of beta particles and resolved the spin-statistics crisis. This idea was converted by Fermi to a theory [2] on the lines of the successful field theory of quantum electrodynamics. Soon after, Maria Goeppart-Mayer proposed a second order beta decay process, double beta decay [3], which would proceed at a very slow rate with typical half lives 10^{17} years.

Two kinds of double beta decay processes are possible involving the emission of (1) 2 $2\bar{\nu}$ $\bar{\nu}$ antineutrino) or (2) 2 2 , EC2 and ECEC2 where EC is the nuclear electron capture process. EC is possible whenever decay is allowed energetically but the reverse is not always true.

Two Neutrino Double Beta decay

Whenever 2 2 decay is possible it usually has to compete with normal single neutrino beta decay. Since it is a decay process which is much slower, by a factor of about 10^{15}- 10^{20}, than single beta decay the former would be almost impossible to observe in the prolific background of the latter process. It is therefore best observed in those cases where single

Dr. V.M. Datar, Nuclear Physics Division, Bhabha Atomic Research Centre, Trombay, Mumbai 400 085;
E-mail: datar@barc.gov.in

neutrino beta decay is energetically forbidden (see Fig. 1).

The first attempts to measure double beta decay (DBD) used geochemical methods following Pontecorvo's suggestion [4]. The idea was to look for an enhancement in the abundance of ^{130}Xe compared to ^{128}Xe, in geologically old samples of tellurium ore, due to the larger phase space for the DBD of the ^{130}Te compared to ^{128}Te. Interpreting absolute concentrations could be misleading so ratios of the xenon isotopes ^{128}Xe/^{132}Xe and ^{130}Xe/^{132}Xe, were measured and led to the first lower limits on DBD half-lives [5]. These were much improved in recent times [6]. The first laboratory real-time observation of 2 2 decay was made by Elliott et al. [7]. Several cases of 2 2 decay have

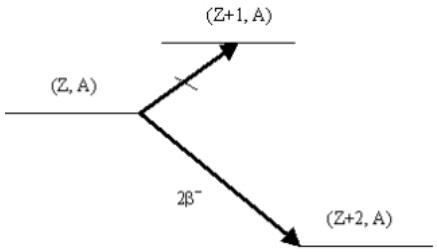

Fig. 1 A typical level diagram for a nucleus undergoing 2 decay. Here decay is energetically forbidden.

since been observed [8], many by the Neutrino Ettore Majorana Observatory (NEMO) collaboration [9].

The DBD decay width $_{2\ 2}$ depends on a phase space factor and a nuclear matrix element (NME) as

$$_{2\ 2} = G(Q\ , Z)\ \ M_2\ \ ^2$$

where G is the phase space factor (approximately Q ^{9} where the latter is the mass difference between the parent and daughter atom) and M_2 the NME. The latter can only be estimated to a factor 3 implying an uncertainty of 10 in the half life.

The qualitative nature of the sum energy spectrum of the two beta particles emitted in DBD is shown in Fig. 2. The DBD spectrum is continuous

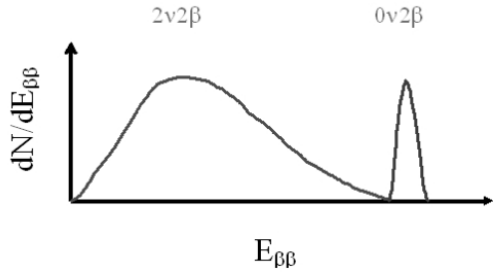

Fig. 2 A typical sum energy spectrum of the two beta particles emitted in DBD and NDBD (neutrino less DBD).

with a maximum energy, known as the end point energy, of Q .

The 2 2 is hampered by the fact that the relevant mass differences are such that the available energies are < 1 MeV with the corresponding values higher by 1.02 and 2.04 MeV, respectively, for EC2 and ECEC2 decays. We will not consider these decays further in this article although searches for these processes, though more difficult, are of great interest.

Zero neutrino or Neutrinoless Double Beta decay

This decay process is of fundamental interest since it may be the only way we might be able to identify the true nature of the neutrino viz. whether it is its own anti-particle (Majorana particle) or is different from its anti-particle (Dirac particle). The possibility of a Majorana nature [10] exists only for neutral spin half (or spin 3/2 etc.) particles.

Nuclei that can decay by 2 DBD can also decay by 0 DBD. However this process involves the emission, in the intermediate state, of a neutrino by a nucleon and its absorption on another nucleon. As mentioned above this can only occur if the neutrino is a Majorana particle. For example, if a neutron emits a right handed neutrino it can be absorbed by a proton if it is left handed. This is not possible in the presently accepted Standard Model if the neutrino is massless. This probability is proportional to a factor (1-) where is the speed of the neutrino in units of the speed of light. In fact it is likely that neutrinoless double beta decay (NDBD) is the only way of probing the Majorana nature of the neutrino in the foreseeable future. For the NDBD

TABLE 1. List of nuclei where 2 2 /2 0 DBD measurements have been made.

Parent Nucleus	Abundance (%)	Q (MeV)	2 2 half-life (years) 1 error	2 0 half-life (years) 90% Confidence level
2 2				
^{48}Ca	0.187	4271.0 4.0	(4.4 0.5) 10^{19}	> 5.8 10^{22} [17]
^{76}Ge	7.8	2039.6 0.9	(1.5 0.1) 10^{21}	> 1.9 10^{25} [11] (2.23± 0.45) 10^{25} 1
^{82}Se	9.2	2995.0 6.0	(9.2 0.7) 10^{19}	> 2.1 10^{21}
^{96}Zr	2.8	3350.0 3.0	(2.0 0.3) 10^{19}	
^{100}Mo	9.6	3034.0 6.0	(7.1 0.5) 10^{18}	> 5.8 10^{23} [9]
^{116}Cd	7.5	2802.0 4.0	(3.0 0.2) 10^{19}	> 1.7 10^{23}
^{128}Te	31.7	868.0 4.0	(2.5 0.3) 10^{24}	> 7.7 10^{24} [6]
^{130}Te	34.5	2533.0 4.0	(9.0 1.0) 10^{20}	> 3.0 10^{24} [16]
^{136}Xe	8.9	2479.0 8.0		> 4.5 10^{23}
^{150}Nd	5.6	3367.1 2.2	(9.1 0.7) 10^{18}	> 3.6 10^{21}
^{238}U	99.275	1145.8 1.7	(2.0 0.6) 10^{21}	
EC 2 -bar				
^{106}Cd	1.25	2771 8	> 3.7 10^{20}	
^{130}Ba	0.106	2611 7	(2.2 0.5) 10^{21}	

events a narrow peak in the sum energy spectrum of the two beta particles at Q is the distinctive signature. A typical spectrum is shown in Fig. 2. The energy spectrum arising from NDBD is a peak at Q . The higher the energy resolution of a detector which measures this sum energy, the better is the ability to distinguish it from the background arising from the tail of the DBD events.

The NDBD decay width is given by the equation

$$_{0\ 2} = G(Q\ , Z)\ M_0\ ^2\ m\ ^2$$

where G is the phase space factor (approximately Q ^{5}), M_0 nuclear matrix element (NME) and m is the effective Majorana mass of the electron neutrino [8]. The phase space factor is Q ^{5} and the nuclear matrix element corresponds to that for 0 2 decay. It is therefore easier to search for this decay process in cases where the Q-value is high. For practical reasons all the nuclei being probed are those with Q > 2 MeV.

Following Avignone et al. [8] the sensitivity to the 0 halflife is given by

$$T_{1/2} = 4.2\ \ 10^{26}\,(\text{yr})\,[\ a/(W n\ )]\ [Mt/(b\ \ (E)]^{1/2}$$

where is the event detection efficiency, a the isotopic abundance, W the molecular weight of the source material, n the number of standard deviations corresponding to a certain needed precision, Mt is the product of the source mass and exposure time, b the background counts and (E) defines the signal region (in the relevant energy

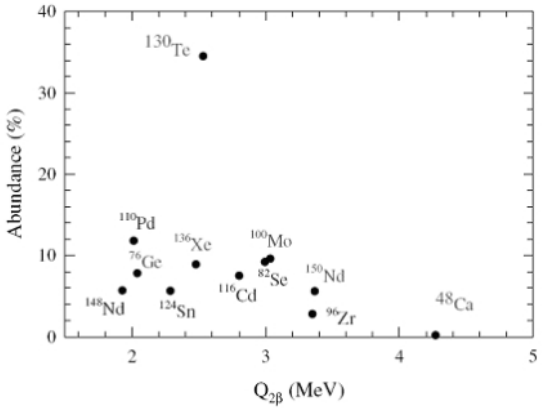

Fig. 3 Natural abundances and Q-values for NDBD candidate nuclei.

domain). It is clear that the lower limit on the NDBD half life can be converted to an upper limit on m and is (Mt) $^{1/4}$. An improvement by a factor of 2 requires an increase in Mt by factor of 16!

There is a variety of techniques that have been used to search for NDBD. The methods broadly use calorimetry, where the total energy deposited by the 2 particles is measured with good energy resolution (up to 0.1% as in high purity germanium detectors enriched in ^{76}Ge), and tracking detectors where energy resolution is poorer but the momenta of the beta particles are measured yielding angular correlation information.

Of the several NDBD candidates (see Fig. 3 below and Table 1) that groups worldwide are working on, a few illustrative examples are briefly described below. Some of the NDBD candidate nuclei have been studied using more than one technique.

The main background in NDBD experiments arises from natural radioactivity from ^{40}K, ^{232}Th and ^{238}U and daughter products from the last two nuclides.

Calorimetric Experiments

^{76}Ge: The first measurements were done with sub kg natural germanium detectors and overground experiments with modest shielding. These were improved upon over the years culminating in the Heidelberg-Moscow experiment [11] done in the underground laboratory at Gran Sasso, Italy and IGEX [12]. The former used 11 kg of enriched ^{76}Ge in 5 HPGe detectors and ran for about 10 years beginning 1990 with good data corresponding to 72 kg.yr. The corresponding numbers for IGEX are 9 kg ^{76}Ge over 8-9 years but with good data for 9 kg.yr. While both collaborations put similar lower limits on a NDBD halflife 2 10^{25} years, translating into an upper limit 0.4 eV/c^2 for the effective Majorana mass m , a part of the Heidelberg-Moscow collaboration have claimed positive evidence for NDBD with a quoted halflife of about 2.2 10^{25} years at 1 implying an m of 0.4 eV/c^2. Efforts are being mounted by the new collaborations GERDA [13] and MAJORANA [14] to either confirm this claim or push the sensitivity to 0.13 eV/c^2 and 0.06 eV/c^2, respectively.

^{130}Te: The first laboratory measurement [15] using a cryogenic bolometer was made by the group of Fiorini at Milano. The basic principle of the method is that the specific heat of a non-magnetic insulator varies as $(T/\ _D)^3$, $_D$ being the Debye temperature, so that if cooled to temperatures 10mK even a small energy deposit of the order of about 2.5 MeV can be measured through a measurable rise in temperature. The temperature sensor is usually a neutron irradiated Ge crystal which has a uniform and large concentration of n- and p-type impurities. For example, in TeO_2 at 10 mK the specific heat is about 0.8 10 ^{13} J/(K mol) leading to a temperature increase 0.5 mK for crystals of about 125 cm^3. The latest results from a scaled up version of the Milano experiment, Cuoricino, used about 41 kg of TeO_2 crystals [16]. The lower limit on the NDBD half life of 1.8 10^{24} years leads to upper bounds on the effective Majorana mass of the neutrino of 0.2 – 1.1 eV/c^2, similar to those from the ^{76}Ge experiments. This experiment is being upgraded to Cuore and will use about 700 kg of TeO_2 with some of it enriched in ^{130}Te.

Tracking Experiments

The NEMO collaboration uses thin metal foils, or powders packed between thin mylar foils, as a beta source, a set of open Geiger Muller counters in a solenoidal magnetic field to track the two electron trajectories and plastic scintillators coupled to

photomultiplier tubes to measure the residual energies for calorimetry. It has measured the 2 DBD half lives of several nuclei and set the lower limit on the NDBD half life of many of these nuclei. The recently completed data runs were based on a version called NEMO-3 which used up to about 10 kg of source material, often enriched, and had energy resolutions (FWHM) of 14-17% at 1 MeV. The planned SuperNEMO upgrade will use up to 200 kg source material and have an improved energy resolution (FWHM) of 7%.

^{100}Mo: A total of about 6.9 kg of enriched ^{100}Mo was used in the form of thin metallic foils. The derived upper limit on m by quoted by NEMO-3 is between 0.6 and 1.3 eV/c^2.

Scintillator Based Experiments

^{48}Ca: An experiment using 23 natural CaF_2(Eu) scintillators, containing about 7.6 gms of ^{48}Ca, was performed by the Osaka group to place a lower bond on the half life for NDBD of ^{48}Ca. While this nucleus has the highest DBD Q-value of about 4.3 MeV, the natural abundance is only 0.19% making enrichment an attractive and even necessary means of improving the sensitivity at 90% confidence level. The present lower limit on the NDBD half life is 5.8 10^{22} years and 3.5 – 22 eV/c^2 [17].

^{136}Xe: Liquid scintillators (LS) have the ability of dissolving upto 2% of Xe. This opens the possibility of measuring the DBD and NDBD in ^{136}Xe especially by using the enriched Xe [18] and large sized LS detectors 100 -1000 tons. An experiment of this nature is planned at Kamioka and Sudbury Neutrino Observatory and is expected to have a sensitivity to m of about 0.1 eV/c^2.

Gas and Liquid Ionization Detectors

^{136}Xe: The EXO detector [19] aims to measure NDBD using an enriched 10 ton gas or liquid phase detector. The detector is a Time Projection Chamber (TPC) which is a position senstive version of an ionization counter with the additional feature that it will tag the daughter ion ^{136}Ba using the laser fluorescence technique. The position sensitivity of the TPC enables the spatial location of the barium ion thereby reducing drastically potential background. The energy resolution is expected to be about 2%. The aimed sensitivity to the NDBD half life is 5 10^{28} years and an m of 10 -50 meV/c^2.

Another experiment is being planned by the XAX collaboration [20] and is much more ambitious in that it hopes to search for DBD, NDBD in ^{136}Xe, weakly interacting massive particles which are candidates of dark matter which is believed to be an important component of the universe and, using a ^{136}Xe depleted $^{129/131}$Xe enriched detector, the energy spectrum of solar pp neutrinos to a precision of 1-2%.

Outlook

In the near future the present generation of experiments, especially the ones based on ^{76}Ge, ^{130}Te, ^{136}Xe and ^{150}Nd should either find evidence for NDBD or push the present upper limit on the effective Majorana mass of 0.5 eV/c^2 down to about 0.05 to 0.1 eV/c^2. Some of these experiments may also shed light on dark matter and make more precise measurements of solar pp neutrinos.

References

1. W. Pauli, letter to participants of workshop at Tubingen Dec. 4, 1930.
2. E. Fermi, Nuovo Cim. 11, 1 (1934); Zeit. f. Phys. 88, 161 (1934).
3. M.Goeppart-Mayer, Phys. Rev. 48, 512 (1935).
4. B. Pontecorvo, Phys. Lett. B 26, 630 (1968).
5. M.G. Inghram and J.K. Reynolds, Phys. Rev. 76, 1265 (1949); ibid 78, 822 (1950) and T. Kirsten et al. Phys. Rev. Lett. 20, 1300 (1968).
6. T. Bernatowicz et al., Phys. Rev. Lett. 69 (1992) 2341; Phys. Rev. C 47, 806 (1993) and references therein.
7. S.R. Elliott, A. Hahn and M. K. Moe, Phys. Rev. Lett. 59, 2020 (1987).
8. F.T. Avignone, S.R. Elliott and J. Engel, Rev. Mod. Phys. 80, 481 (2008).
9. L. Vala on behalf of the NEMO3 and SuperNEMO collaboration, arXiv:0901.0473v1 [hep-ex] 5 Jan 2009; see also the NEMO collaboration website http://nemo.in2p3.fr/

10. E. Majorana, Nuovo Cimento 14, 171 (1937).

11. H. Klapdor-Kleingrothaus. et al., Eur. Phys. J. A 12, 147 (2001); H.V. Klapdor-Kleingrothaus et al., Mod. Phys. Lett. A 16, 2409 (2001). Evidence for NDBD presented by a subset of the Heidelberg-Moscow collaboration: H. V. Klapdor-Kleingrothaus, A. Deitz, I. V. Krivosheina, and O. Chkvorez, Phys. Lett. B 586, 198 (2004) and H. V. Klapdor-Kleingrothaus and I. V. Krivosheina, Mod. Phys. Lett. A 21, 1547 (2006).

12. C.E. Aalseth, Phys. Rev. D 70, 078302 (2004).

13. K.T. Knopfle, inv.talk at ICHEP08, arXiv: 0809.5207v2 and references therein.

14. V.E. Guiseppe, for the Majorana Collaboration, arXiv:0811.2446.

15. E. Fiorini and T. Niinikoski, Nucl. Instr. and Meth. 224, 83 (1984).

16. C. Arnaboldi et al., Phys. Rev. Lett. 95, 142501 (2005) and references therein.

17. S. Umehara et al., Phys.Rev.C78, 058501 (2008); arXiv:0810.4746v1 [nucl-ex] 27 Oct 2008.

18. R.S. Raghavan, Phys. Rev. Lett. 72, 1411 (1994); B.Caccianiga, M. Giammarchi, Astroparticle Phys.14, 15 (2000).

19. K. Wamba for the EXO collaboration, arXiv:hep-ph/0210186v1 12 Oct 2002.

20. K. Arisaka for the XAX collaboration, arXiv:0808.3968v3 [astro-ph] 7 Jan 2009.

Beta-Delayed Particle Emission

Dr. K. Sudarshan *is gold medalist from University of Hyderabad in MSc chemistry in 1998. He joined radiochemistry division of BARC in 1999 from the 42nd batch of training school. He has obtained his PhD degree from Mumbai University in 2008. His research areas include positron annihilation spectroscopy, radio analytical techniques and heavy ion induced reactions. He has published about 30 papers in peer-reviewed journals.*

Beta decay is one of the first forms of radioactivity observed where a nucleus transforms to its neighbouring isobar with conversion of one neutron to proton or proton to neutron. The mass parabola of isobaric series of mass number A=151 is pictorially represented as Fig. 1 [1]. Each point in mass parabola represents the mass of the nuclei in their ground state. No nucleus in its ground state can get rid of energy without changing the number of neutrons or protons. The $^-$ and $^+$ emission and electron capture (EC), together classified as beta decay, is very common mode in which nuclei on the mass parabola decay to their successive neighbours until the valley of stability is reached. It can also be seen from the figure that the beta decay energies (difference between masses of successive atomic number) increase rapidly with distance from the valley of stability. The Q values involved in the beta decays of the nuclei near the stability line are in the range of few MeV while it can be in excess of 10 MeV for the nuclei far away from stability. As an example, inset in Figure 1 shows the available paths for the decay of ^{151}Lu. The first path leads to ground state of ^{151}Yb by simple $^+$ decay, which rarely occurs alone. Often, the beta decay leads to the population of excited states in the daughter nuclei which decay to ground states by emission of gamma-rays. However, as the distance from the stability line increases, the energy difference between successive nuclei is very high. This leads to situations where particle unbound excited states are populated in beta decay and these can emit a wide range of particles. All such decays are generally classified as beta delayed particle emission Experimentally many different types of beta-delayed particles emissions like p, 2p, n, xn, d, t and have been observed. Emission of smaller particles is common and heavier systems would be suppressed due to the coulomb barrier similar to one encountered in cluster emission. In the limit of large masses of the emitted fragment, the process turns into beta-delayed fission, observed in heavy nuclei. The case shown in Fig. 1 corresponds to the excited state of ^{151}Yb which can decay by emitting proton and is called beta delayed proton emission. The other side of the valley of stability in mass parabola is matched by $^-$ delayed neutron emission.

The force responsible for beta decay is called weak force while the force which binds the nucleons together is strong force. This strong force is also responsible for the emission of nucleons from the nuclei when the binding energy is insufficient. So the time scales of particle emission are considerably shorter than the beta decay lifetimes of their precursors and hence usually the observed lifetimes of these particle emissions correspond to the lifetimes of their beta decaying precursors. It should be mentioned that third decay path shown as particle emission from ground state sets the limit of isotope synthesis. If significant amount of energy is gained by direct particle emission then it takes dominance over the beta decay. If the nuclei have to first go through beta decay before particle emission, the lifetimes of the nuclei are longer and make the synthesis and identification of those nuclei possible. In some cases where the nuclei are unstable towards charge particle decay, the nuclei were separated and their properties measured as the lifetimes are longer owing to coulomb barrier [1].

Dr. K. Sudarshan, Radiochemistry Division, Bhabha Atomic Research Centre, Mumbai 400 085;
E-mail: kaths@barc.gov.in

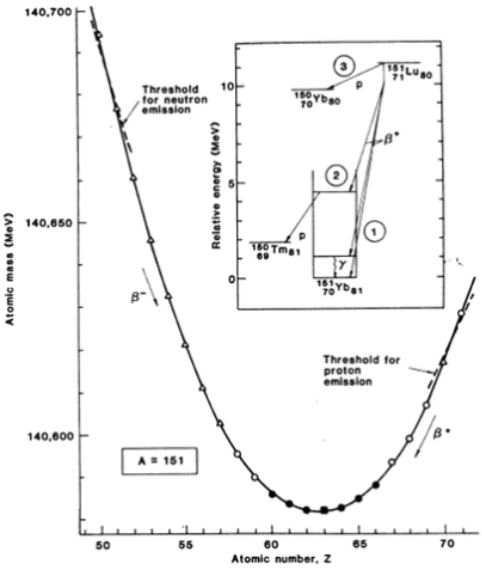

Fig. 1 Atomic masses of a series of isotopes that have 151 nucleons (A = 151). The filled and open symbols correspond to measured and predicted masses respectively. The masses are given in energy units (MeV) to emphasize the energy released by decay between neighboring nuclei. The only stable isotope, ^{151}Eu, is shown as a darkened square. The dashed lines show the approximate threshold at which a neutron or proton becomes energetically unbound by the nucleus. The inset illustrates three possible decay channels for the very neutron-deficient nucleus ^{151}Lu [1].

The Q-value for -delayed emission of x number of neutrons from the nucleus of mass (A, Z) can be written as

$$Q_{-xn} \quad Q_{-} \quad S_{xn} \quad {}^{A}(Z \quad 1) = Q_{-} \quad {}^{A-x}Z \quad S_{xn}$$

The first expression involves the Q-value of the parent nucleus and the separation energies of the beta-daughter, but it can be written also in terms of the separation energies of the mother nucleus and the Q-value of a lighter isotope [2]. A related formula applies to $^{+}$-delayed emission of protons, one can replace Q_{-} by Q_{EC} and use that $Q_{-} = Q_{EC} - 2\ m_e c^2$ The Q-value for other delayed particle-emissions can be rewritten in the general form $Q_x = C - S$ where the constants C and "separation energies" S for the different processes are given in Table 1 (all separation energies refer to the mother nucleus (A,Z) for delayed -emission a Q-value for the final nucleus enters).

TABLE 1. Parameters in the Q-values equation for nucleus $^{A}_{Z}$

x	C (keV)	S
$^{-}$p	782	S_n
$^{-}$d	3007	S_{2n}
$^{-}$t	9264	S_{3n}
$^{-}$	29860	$S_{4n} + Q\ (^{A-4}_{Z-1})$
ECn	-782	S_p
ECd	1442	S_{2p}
EC ^{3}He	6936	S_{3p}
EC	26731	$S_{4p} + Q_{EC}(^{A-4}_{Z-3})$

As seen from the formulae, the deciding factors in the positive Q-values of beta delayed emission of particles are the separation energies. So these processes are more predominant in the nuclei near the driplines where the separation energies are very small. The nuclei in lower mass region which have positive Q-values for beta delayed emission are shown in Fig. 2 [3].

Though very neutron rich isotopes decay by $^{-}$ delayed neutron/neutrons emission and neutron deficient isotopes by $^{+}$/EC delayed proton emission, it is not necessary a nuclei can emit only one kind of beta delayed particle. One such example is the case of ^{11}Li which shows different beta delayed particle emissions as given below.

$^{11}_{3}Li_{8}$ $\quad$ $^{11}_{4}Be_{7}$ $\quad$ (12%)

$^{10}_{4}Be_{6}$ $\quad$ n $\quad$ (81%)

$^{10}_{4}Be_{5}$ $\quad$ 2n $\quad$ (4%)

$^{8}_{3}Li_{5}$ $\quad$ t $\quad$ (0.01%)

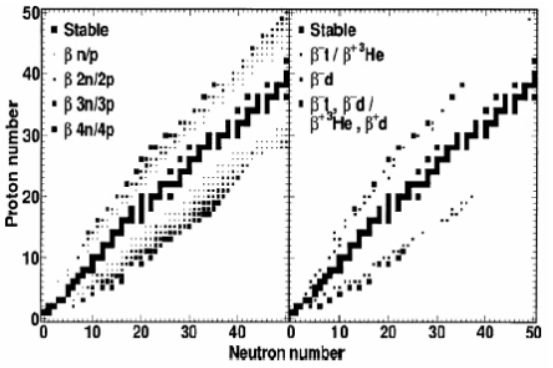

Fig. 2 *Nuclei with N, Z 50 for which the Q-value for various -delayed particle emission processes is positive. The left half shows single- and multi-nucleon emission and the right, emission of nuclei of mass number 2 and 3.*

$^{6}_{2}He_{4}$ n (1%)
$^{4}_{2}He_{2}$ 3n (2%)

As most of the nuclei showing these exotic decay modes lie close to the driplines and are short lived, the production and identification of nuclei and measuring the various possible decay modes is a challenging task. For a long time, thermal neutron induced fission has been source of neutron rich exotic nuclei. Later, deep inelastic heavy ion reactions provided a new way producing these isotopes. With the advancement of facilities producing very high energy projectiles, the projectile fragmentation has become an important route to produce these isotopes and study their decay properties. Due to high energies involved, the kinematics focussing of the fragments is well suited for magnetic separation procedures. The advancements in the high efficient and rapid separation processes of these fragments have enhanced the number of nuclei studied for the various exotic decays.

As discussed earlier, in the exotic decay of nuclei called beta delayed particle emission, the particles such as p, 2p, n, xn, d, t and have been observed. For simplicity the various beta delayed particles emissions would be discussed in the following sections under categories: beta delayed single nucleon emission (neutron or proton) processes, multi nucleon (xn, 2p) emission processes, composite nucleus emission (, ^{3}He, t, d) processes and delayed fission.

Beta Delayed Neutron and Proton Emission

The $^{-}$ delayed emission of neutrons in the neutron rich fission products with low neutron binding energies has been well documented. The neutrons are promptly emitted but the overall time scale is governed by the beta decay of the delayed neutron precursor. Because of the importance of delayed neutrons in the reactor control, the delayed emission in fission products has been extensively studied. The beta delayed neutron emission rates also play an important role in understanding the isobaric distribution of nucleus in the r-processes [4]. The delayed neutron emission probabilities depend strongly on the total energy available in the beta decay of the precursor (Q) and neutron separation energies of the neutron emitter (S_n). Since the neutron emission occurs from a region of high level density, the beta decay to these levels can be treated statistically. Assuming the beta strength function to be constant above a cut of energy C and zero below it, the delayed emission probabilities can be approximated as [n=5]

$$P_n \quad \frac{Q_{-} \quad S_n}{Q_{-} \quad C}^{n \ 1}$$

The total neutron emission probabilities in different Na and Mg isotopes are shown in Fig. 3 [5-7]. Unmoderated neutron detection methods have limited efficiencies and the exact neutron energy spectra are difficult to measure experimentally. The integrated $^{-}$- dealyed neutron emission is usually measured. This information is essential to evaluate the level of competition taking place between neutron capture and -decay for those neutron-rich nuclei of importance to the astrophysical r-process.

The $^{-}$-delayed neutron emission and $^{+}$-delayed proton emission are charge symmetric. The production and measurement of properties of nuclei with no neutron binding energies (dripline nuclei) in the ground state is difficult as the neutrons face no barrier for emission while the nuclei with

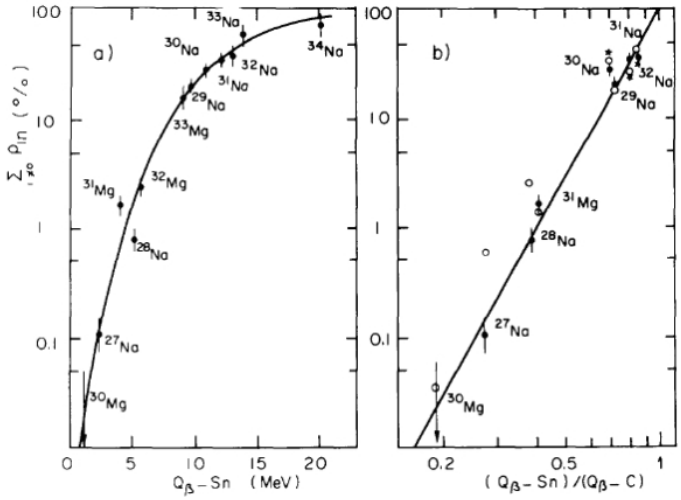

Fig. 3 *(a) Systematics of $\sum_{i=1}^{n} P_{in}$ for Na and Mg isotopes relative to Q -S_n values. The solid line is drawn to guide the eye. (b) Variation of $\sum_{i=1}^{n} P_{in}$ with the ratio (Q -S_n)/(Q -C) for all Na and Mg -delayed neutron emitters with known -decay scheme. C is taken as the excitation energy of the first -fed level.*

proton unbound ground states still can be identified in favourable cases as they face the coulomb barrier for proton emission. The study of these delayed nucleon emission assumes importance in understanding the interplay of various forces that determine these decay processes [8]. Exact measurement of the proton energies in $^{+}$- delayed proton decays is easier and allows precise level-by-level spectroscopy in neutron-deficient nuclei. The beta delayed proton decay has been used to test the theoretical predictions of the -decay rates. Some typical beta-delayed proton emitters and branching fractions are given in Table.2a. However, it may be pointed out the there are many nuclei with Z<N also showing the beta delayed emission of protons and few examples are given in Table 2b. However, these precursors have very low proton branching ratio as compared to the proton rich nuclei [9].

Delayed Multi Particle Emission

In the beta delayed multi particle emission, the nucleus breaks into more than two particles. In many nuclei, the pairing energy makes many even Z nuclei stable towards single nucleon emission and unstable towards two neutron or proton emissions. The beta delayed emission of more than one neutron and protons are observed in many nuclei [10, 11]. The delayed emission of combination of protons and neutrons is less common than the emission of their composite particles. The kinematics of the particles is decided by energy and momentum conservations. The main interest in -delayed multi-particle emission is the fact that the mechanism of the break-up is not fully determined by energy and momentum conservation. In three body break-up there are three binary subsystems and each subsystem have resonances controlling the break-up. Whether the break-up proceeds via each of these resonances sequentially or the beta-daughter breaks up directly into the three body continuum is still a matter of investigation. Sequential and direct break-up represent limiting multi-particle mechanisms as direct processes and compound nucleus are for nuclear-reaction mechanisms. The observation of the emission of more than one nucleon also provides information on the formation of such clusters in nuclei.

The mechanism of multiparticle emission, whether it is simultaneous emission or sequential can be studied by observing the energy and angular correlations of these particles. The beta delayed two-proton emission has been used for this purpose.

TABLE 2a. Some proton rich nuclei showing delayed proton emission

Precursor	Production reaction[a]	$t_{1/2}$ (msec)	Q -B_p (MeV)[b]	Proton branching ratio
N odd				
$^{9}_{6}C_{3}$	^{10}B (p,2n)	127 1	16.68	~1.0
$^{13}_{8}O_{5}$	^{14}N (p,2n)	8.9 0.2	15.82	0.12
$^{17}_{10}Ne_{7}$	^{16}O (^{3}He, 2n)	109 1	13.93	0.99
$^{21}_{12}Mg_{9}$	^{20}Ne (^{3}He, 2n)	123 3	10.67	0.33
$^{25}_{14}Si_{11}$	^{24}Mg (^{3}He, 2n)	221 3	10.47	0.32
$^{29}_{16}S_{13}$	^{28}Si (^{3}He, 2n)	188 4	11.04	0.47
$^{33}_{18}Ar_{15}$	^{32}S (^{3}He, 2n)	174 2	9.34	0.34
$^{37}_{20}Ca_{17}$	^{36}Ar (^{3}He, 2n)	175 3	9.78	0.76
$^{41}_{22}Ti_{19}$	^{40}Ca (^{3}He, 2n)	80 2	11.77	1.0
$^{45}_{24}Cr_{21}$	^{32}S (^{16}O,3n)	50 6	10.80	0.25
$^{49}_{26}Fe_{23}$	^{40}Ca (^{12}C, 3n)	75 10	11.00	0.60
$^{53}_{28}Ni_{25}$	^{40}Ca (^{16}O, 3n)	45 15	11.63	0.45
$^{57}_{30}Zn_{27}$	^{40}Ca (^{20}Ne, 3n)	40 10	13.99	0.65
$^{61}_{32}Ge_{29}$	^{40}Ca (^{24}Mg, 3n)	~40	~12.2	~0.50

TABLE 2b. Some -delayed proton emitters with Z<N

Precursor	Production reaction[a]	$t_{1/2}$ (sec)	Q -B_p (MeV)	Proton branching ratio
$^{109}_{52}Te_{57}$	^{96}Ru (^{16}O, 3n)	4.4 0.4	7.14	~3.0 x 10^{-2}
$^{111}_{52}Te_{59}$	^{102}Pd (^{12}C, 3n)	19.3 0.4	5.07	~1.0 x 10^{-3}
$^{113}_{54}Xe_{59}$	Ce (p, 5pXn)	2.8 0.2	7.09[c]	~4.0 x 10^{-2}
$^{115}_{54}Xe_{61}$	Ce (p, 5pXn)	18.0 3.0	6.20	3.4 x 10^{-3}
$^{117}_{54}Xe_{63}$	Ce (p, 5pXn)	65.0 6.0	4.10	2.9 x 10^{-5}
$^{114}_{55}Cs_{59}$	La (p, 3pXn)	0.7 0.2	8.20[c]	
$^{116}_{55}Cs_{61}$	La (p, 3pXn)	3.6 0.2	6.43	2.7 x 10^{-3}
$^{118}_{55}Cs_{63}$	La (p, 3pXn)	16.4 1.2	4.70	4.2 x 10^{-4}
$^{120}_{55}Cs_{65}$	La (p, 3pXn)	58.3 1.8	2.65[c]	7.0 x 10^{-8}
$^{117}_{56}Ba_{61}$	^{92}Mo (^{32}S,2p5n)	1.9 0.2	8.08[c]	
$^{119}_{56}Ba_{63}$	^{92}Mo (^{32}S,2p3n)	5.3 0.3	6.35	9.0 x 10^{-3}
$^{121}_{56}Ba_{65}$	^{92}Mo (^{32}S,2pn)	29.7 1.5	4.70	2.0 x 10^{-4}

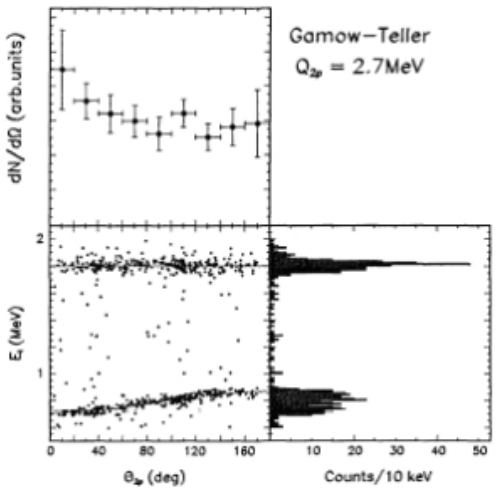

Fig. 4 The distribution of individual proton energies and the angle between them for the 2.7 MeV Q_{2p}-peak. This corresponds to the 2p-transition from a GT-fed state in ^{31}C1 at 7.36 MeV ending in the g.s. of ^{29}P. The angular distribution shows a small angular dependence typical of a sequential decay [12].

The studies so far point to the sequential emission of two protons in $^{+}$-2p decay as indicated by little or no angular correlations between the emitted particles as shown in $^{+}$-2p decay of ^{31}Cl [12] as shown in Fig.4.

Composite Particle Emission

The synthesis of nuclei farther from stability line with enormously large Q values opens further exotic decay modes. One such example is beta delayed emission of ^{3}He, and tritons besides neutrons in the decay of ^{11}Li. Emission of such composite particles is possible in many other nuclei and delayed emission of alpha particles is reported in many nuclei [13-15]. These states are situated typically at 5-12 MeV excitation energy and are thus bridging the gap between, on the one hand, the ground states, which in certain cases show alpha radioactivity, and on the other hand the compound nuclear states near or above the Coulomb barrier, accessible through reaction processes. The study of the beta delayed emission of composite particles is expected to throw light on the formation probabilities of alpha and other composite particles in a relatively cold nucleus. The proton rich isotopes of Te, I, Xe, and Cs showing the delayed alpha emission are shown in the Fig. 5 [16]. In many nuclei, the beta delayed proton decay competes with the delayed alpha decay.

Delayed Fission

The beta delayed fission may also be treated as extreme case of particle emission. The beta delayed fission can be represented as

$$(N,Z) \qquad (N \quad 1, Z \mp 1) \qquad \underset{i}{(N_i, Z_i)}$$

where the N_i and Z_i refers to the neutron number and proton number respectively, of the fission product and the asterisk indicates the excited state populated in beta decay. To observe considerable beta delayed fission branching in the nuclei, the beta decay half-lives should be shorter than the alpha or spontaneous fission half lives of the parent. i.e. the beta decay should be one of the major branches of decay and the decay Q values should be higher than the fission barrier of the daughter nucleus. The neutron rich nuclei which are expected and observed to show beta delayed fission are shown in Fig.6 [17]. The graph shown here is rather old. Delayed fission has been already established in many of nuclides shown in the region 2 (expected to show delayed fission based on calculations) [18]. The proton rich nuclei which have shown and expected to show the beta delayed fission are also shown as open and closed circles. The fission induced by neutrons has been most studied area in the low energy fission. The delayed fission also provides useful information on the low energy fission of nuclides. The beta delayed fission has been used in determining fission barriers in many nuclei [19]. Since, the heavy elements are formed in the nucleosynthesis by successive neutron capture and beta decay, all the beta delayed particle emissions play pivotal role in deciding the final composition of the elements and their study is necessary to understand various processes and problems in astrophysics [20].

Significant developments in the production and separation of nuclei far from valley of stability have increased the scope of studying the nuclei with exotic decay modes as beta delayed particle emission. The developments have been significant

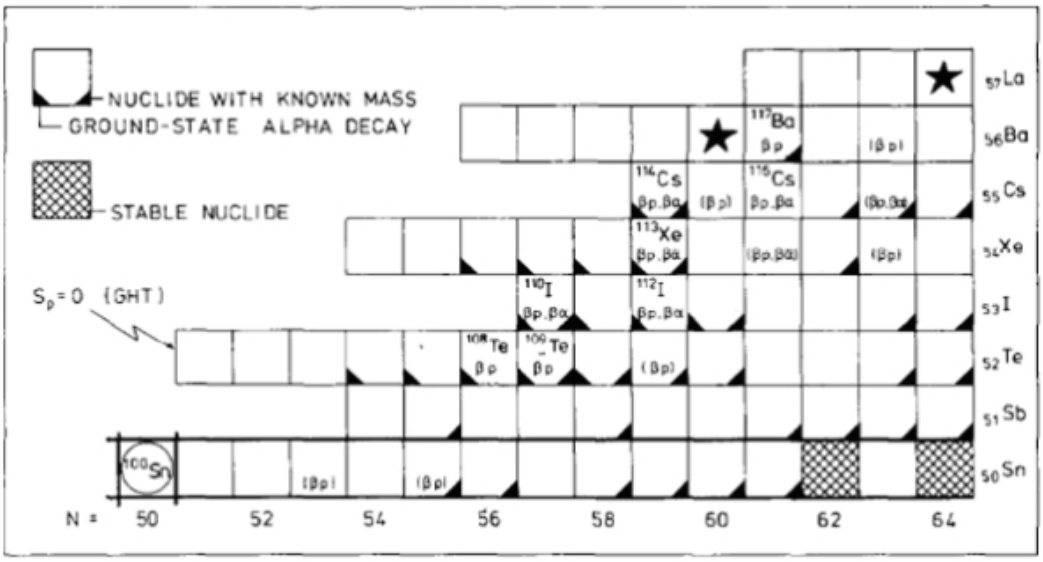

Fig. 5 A section of the nuclide chart with representative nuclides showing beta-delayed proton and alpha particle emission [12]

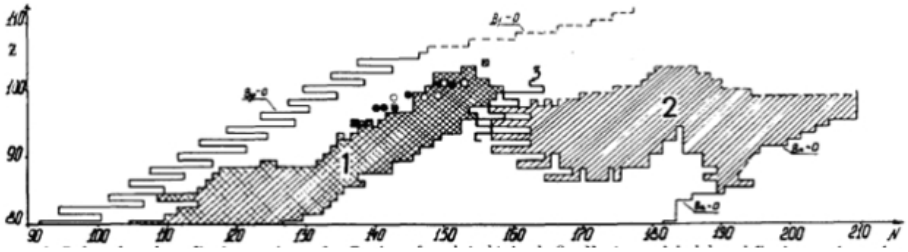

Fig. 6 Delayed nuclear fission regions: 1 - Region of nuclei obtained; 2 – Expected neutron-rich delayed fission region calculated from mass values. 3 - Boundary of neutron-rich delayed fission region calculated [17].

especially in lighter mass region where the separation techniques have reigned supreme. The complexities associated with beta delayed multiparticle emissions require sophisticated instrumentation to decipher information unequivocally. The complexities in the beta delayed multiparticle emission and other exotic decay modes are exemplified in the decay scheme of ^{31}Ar in Fig. 7. Many nuclei with predicted beta delayed particle emissions are yet to be observed. The advancements in the high intensity radioactive ion beams and nuclear instrumentation are expected to provide the opportunity to study many more such isotopes which would give further insight into the nuclear structure and unanswered questions in astrophysics.

References

1. J.C. Hardy, Science 227, No. 4690 (1985) 993.
2. K. Riisager, Eur. Phys. J. A. 15 (2002) 75.
3. B. Jonson and K. Riisager, Nucl. Phys. A. 693 (2001) 77.
4. F. Montes et al., Phys. Rev. C 73 (2006) 035801.
5. K.L. Kratz and G. Herrmann, Z. Phys. 263 (1973) 435.

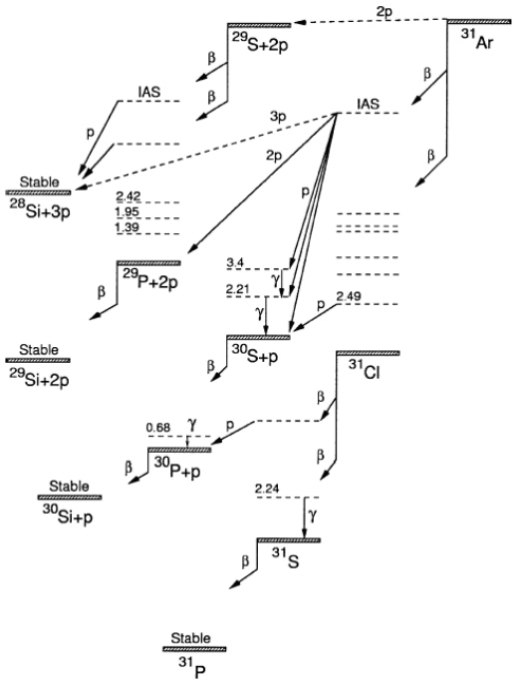

Fig. 7 Decay scheme of ^{31}Ar and its daughters. This figure shows the complexities in the beta decay of an exotic nucleus. Note that ^{31}Ar could be two-proton radioactive, but neither this branch nor the beta-delayed three-proton branches have been established experimentally [3].

6. M. Langevin et al., Nucl. Phys. A. 414 (1984) 151.
7. K. Takahanashi, Prog. Theor. Phys. 47 (1972) 1500.
8. C. Detraz, D. J. Vieira, Ann. Rev. Nucl. Part. Sci. 39 (1989) 407.
9. J. Cerny, J.C. Hardy, Ann. Rev. Nucl. Sci. 27 (1977) 333.
10. J.P. Dufour et al., Phys. Lett. B. 206 (1998) 195.
11. B. Blank et al., Nucl. Phys. A. 615 (1997) 52.
12. M.J.G. Borge et al, in International Nuclear Physics Conference INPC 2001, Edited by E. Norman et al., CP610.
13. P. Hornshoj et al., Phys. Lett. B. 55 (1975) 53.
14. B. Blank, J. Phys. G.: Nucl. Part. Phys. 24 (1998) 1385
15. H. Jeppesen et al. Prog. Theor. Phys. Suppl. 146 (2002) 520.
16. P.T. Petersson et al., Nucl Phys. A. 437 (1985) 342
17. E. Ye. Berlovich and Yu. N. Novikov, Phys. Lett. B 29 (1969) 155.
18. D. Habs et al., Z. Phys. A. 285 (1978) 53.
19. H.V. Klapdor et al., Z. Phys. A 292 (1979) 249.
20. F.-K. Thielemann et al., Z. Phys. A 309 (1983) 301.

Non-Nucleonic Excitations in Nuclei

Dr. A.B. Santra *joined BARC in 1978 after doing M.Sc. in Physics from IIT Kharagpur; subsequently did Ph.D. and post-doctoral work from University of Mumbai and University of Alberta, Canada respectively. His research interest mainly lies in the interface areas of nuclear and particle physics. He worked on resonance excitations in nuclear reactions, weak decays of heavy mesons, structure of neutron stars and nuclear matter. Currently, he is interested in understanding problems of low energy nuclear physics, saturation of nuclear matter in particular, including effects arising from the fundamental dynamics of strong interaction.*

Abstract

Nuclei are complex-composite systems. Characteristic to such systems nuclei exhibit a very rich excitation energy spectrum. These could involve usual nucleonic or non-nucleonic degrees of freedom, depending on the energy scale. Non-nucleonic degrees of freedom include various mesonic and baryonic resonances. In this article, we aim to discuss excitations of non-nucleonic degrees of freedom from the quark dynamics. An exotic state called "pentaquark" is discussed to show how observation of such a state may open a new direction towards understanding the strong interaction dynamics.

Introduction

The atomic nucleus is a bound system of neutrons (n) and protons (p) interacting through strong interaction. Neutron and proton have mass about 939 MeV, and behave identically in strong interactions. These are considered to be two isotopic spin projections of a state called nucleon with isotopic spin 1/2. The isotopic spin (or isospin) is conserved in strong interaction. The group of strongly interacting fermions (half integral spin) is called baryons. Nucleons are baryons with baryon number (B) one.

It was realized quite early that nuclei are far more complex than just collection of neutrons and protons. As early as in 1935, Yukawa proposed the idea that nucleons interact through the exchange of a boson (integral spin particles) of mass about 140 MeV. Such a particle with spin-zero was discovered later and named pion . It appears in three charge states, namely, $^{+}$, ^{0} and $^{-}$ with almost same masses of about 140 MeV. These three charge states behave identically in strong interaction, so pion is assigned isospin one. The group of strongly interacting bosons is called mesons. Meson number need not be conserved in a nuclear interaction. Pion is the lightest member of meson group.

Over the years, this interaction mechanism has been extended to include the exchange of heavier members of the meson group, such as sigma ( ), rho ( ), omega ( ), eta ( ) and others between nucleons. The two nucleon interacting potential, obtained invoking meson exchange mechanism between nucleons, is able to account extremely well all data of nucleon-nucleon scattering experiments up to about 400 MeV. Thus, there must be various mesons present in a nucleus for binding the nucleons together to form the nucleus.

However, in spite of this very strong theoretical reason to expect mesons in the nucleus, it was not easy experimentally to isolate the effects arising from these mesonic constituents. It was even more difficult to see their presence directly. The clear evidence indicating presence of mesonic effects was found in the radiative capture of thermal neutrons in hydrogen, n + p d + . Experimentally, the cross-section is 334.2 0.5 mb, whereas the best calculations taking only nucleonic degrees of freedom give about 302.5 mb. This discrepancy of about 10% is now reasonably well understood in terms of effects arising due to non-nucleonic or mesonic degrees of freedom.

Dr. A.B.Santra, Nuclear Physics Division, Bhabha Atomic Research Centre, Trombay, Mumbai 400 085:
E-mail: santra@barc.gov.in

There are several types of non-nucleonic excitations in nuclei. Excitation of such degrees of freedom in nuclei gives crucial information towards understanding of the basic dynamics of strong interaction. Here, we aim to discuss about two different types of non-nucleonic excitations. This article is organised as follows: We discuss In section (2) about the structure of the nucleons the building blocks of nuclei, in section (3) about the strong interaction from the fundamental point of view, in section (4), about excitations of free resonances, in section (5) about the mechanism of modification of resonances in nuclei, in section (6) about a new type of excitation called pentaquark. Lastly in section (7) we give a summary of the article.

Structure of Nucleon

Magnetic moment of a structure-less point-like spin 1/2 particle with mass m and charge e is $e\hbar/2m$. Neutron and proton are thus expected to have magnetic moments 0 and 1 nuclear magneton respectively. However, observed magnetic moments of neutron are -1.91 and that of proton is 2.79 nuclear magneton. Nucleons are not structure-less point-like particles.

First experimental evidence towards internal structure of nucleon was obtained in the 1950's in $^{+}$ and $^{-}$ scattering off the proton [1]. The scattering cross-section, when plotted as a function of total energy, shows a broad resonance like structure, which is due to the formation of an intermediate state, called delta ( ), the lowest excited state of nucleon. The mass of ( )is 1232 MeV and the width is about 112 MeV. It decays predominantly through the strong interaction to pion and nucleon with lifetime of the order of 5×10^{-24} sec corresponding to the decay width. The spin and isotopic spin of this state have been identified to be 3/2 and 3/2 respectively.

Within a few years after the discovery of delta, a large number of short lived strongly interacting particles, usually called resonances, were discovered. Besides the excited states of nucleons, these resonances included particles that show "strange" behavior. These were produced copiously but decayed slowly. Noting that production of these particles always associated pairs, a new conserved quantity, called "strangeness", was postulated. Strangeness was preserved during their creation, but not conserved in their decay. The production of these particles is via strong interaction that conserves "strangeness", and decay is through "strangeness" violating weak interaction.

Existence of conserved quantities in an interaction is always associated with some symmetry of the interaction. The set of symmetry transformations constitute a "group". Gell-Mann [2] identified the symmetry group corresponding to the symmetry that conserves isospin and strangeness to be SU(3), the group of 3-dimensional unitary matrices of determinant one. He recognized that this symmetry group could generate natural groupings of hadrons (strongly interacting particles), mesons and baryons together into sets with same spin and parity consisting of particles of isospin (I) multiplets that differ only by strangeness (S). For example, the baryon octet consists of, (I=1/2, S=0) two nucleons, (I = 1, S = -1) three sigma ( ), (I = 0, S = -1) one lambda ( ) and (I = 1/2, S = -2) two cascade ( ). The group of particles with same spin and parity actually correspond to the states of representation space of the SU(3) group. The members of the baryon octet mentioned above correspond to the states of eight dimensional representation of SU(3) group. The fundamental representation of SU(3) is three dimensional, and higher dimensional representations of SU(3) can be constructed from the fundamental representation. Strangely enough, none of the observed groups particles ever corresponded to the fundamental representation of SU(3). This indicates the existence of a deeper level of elementary constituents of matter. The particles corresponding to higher dimensional representation of SU(3) must be composed of those corresponding to the fundamental three dimensional representation of SU(3)!

In 1964 Gell-Mann and Zweig [3] proposed the idea of quarks as the constituents of hadrons. It is possible to understand all low lying hadrons with only three spin 1/2 quarks, up (u), down (d) and strange (s).

Quark	Charge (Q)	I	I_Z	S	Baryon No. (B)
u	2/3	1/2	1/2	0	1/3

d	-1/3	1/2	-1/2	0	1/3
s	-1/3	0		-1	1/3

Different types of quark are termed as flavors, which is conserved in strong interaction but not in weak interaction. Later three more flavors of quark, namely, charm, beauty and top, have been discovered. According to relativistic quantum mechanics, corresponding to every particle there must exist an antiparticle with same mass and opposite charge. Quarks (q) are thus associated with anti-quarks ($\bar{q}$). The baryons are composed of three quarks (q) to make, B = 1, and the mesons are with a pair of quark (q) and antiquark ($\bar{q}$) to make B = 0.

Quark structures of a few baryons and mesons can be written as, p (uud), n (udd), $^{+++}$ (uuu), $^{+}$ (uud$\bar{d}$), ^{0} (udd$\bar{d}$), $^{-}$ (ddd$\bar{d}$), $^{+}$ (ud$\bar{d}$), ^{0} (uu-dd$\bar{d}$)/$\sqrt{2}$, $^{-}$ (du$\bar{u}$), K^{+} (us$\bar{u}$), K^{-} (su$\bar{u}$), $^{+}$ (uus$\bar{d}$), $^{-}$ (dds$\bar{u}$), ^{0} (uds$\bar{u}$). There is a one to one correspondence between the observed hadrons and the states predicted by this simple classification; thus, the quark model appears to be a very useful periodic table of hadrons.

In the late 1960's Friedman, Kendall and Taylor [4] discovered quarks in their pioneering experiment, by hitting the proton hard with electron in the deep inelastic region where the energy transfer ( ) and the momentum transfer (Q) are very large. At high momentum and energy transfer the elastic collisions become very unlikely, as elastic form factor decreases rapidly. However, the proton was found to break up into hadron fragments. The inelastic cross-section is very large! Proton must be made of something more elementary. The quark model of Gellman and Zweig got experimental confirmation.

The observed structure functions of electron-proton scattering in the deep inelastic region showed a very peculiar property. These depend only on one variable, $x = Q^2/2M$, (with M as the proton mass) instead of Q^2 and separately. This is known as Bjorken scaling [5], and this can be understood only by considering the proton to be composed of point-like, non-interacting, spin-half particles.

The understandings of hadrons in terms of quarks face a problem concerning the Fermi-Dirac statistics of the constituents. Since the fundamental state of a composite system is expected to have zero oribital angular momentum, the $^{++}$ baryon (J = 3/2) corresponds to (u u u), with the three quark-spins aligned in the same direction and all relative angular momentum equal to zero. This wave function is symmetric and, therefore, the $^{++}$ state obeys the wrong statistics. The problem can be solved [6] by assuming the existence of a new quantum number called, color, such that each species of quark may have three different colors, say (red, yellow, green). One can construct an anti-symmetric state of the $^{++}$ in which the colour part of the wavefunction is antisymmetric. At least three colors are needed for making an antisymmetric state. Baryons and mesons are described by the color-singlet combinations of quarks. Direct test of the color quantum number, however, has been obtained through various processes, and number of colors has been experimentally determined to be three.

States with non-zero color have not been observed. So, it is further postulated that all asymptotic states are colorless, i.e. singlets under rotations in color space. This assumption is known as the confinement hypothesis, because it implies the non-observability of free quarks: since quarks carry color they are confined within color-singlet bound states.

Strong Interaction

The baryons and mesons are made of quarks. The strong interaction that binds nucleons to form nuclei must be some kind of residual manifestation of the strong interaction among quarks. The strong interactions of quarks are due to their "color" charges. There must be an object to exchange color charge from one quark to the other. Each quark carries three types of color charge, so, nine different colored objects would be required to make all possible change of colors of quarks. However, from these nine, it is possible to make a combination which is color neutral and would combine with any color in the same way. Excluding that one we get eight objects to mediate strong interaction between quarks. These are called gluons, which are spin-1

bosons and massless. In electromagnetic interaction there is only one neutral photon that mediates the interaction. In contrast, in case of strong interaction there are eight gluons which are colored. The interaction of quarks by exchanging gluons is described by a theory, modeled in the similar framework of electromagnetic interaction, is called quantum chromodynamics, or QCD. It is a quantum field theory in which interaction between quark and gluon is introduced using the principle of local gauge invariance [7].

One of the most important wisdom of relativistic quantum theory is that, the vacuum is not just the empty space; it can be thought of as a medium of virtual particles. In QCD the vacuum contains virtual quark-antiquark pairs that interact by exchanging virtual gluons. When a quark is placed in vacuum, its color can polarize this medium of virtual quark-antiquark and gluon, and due to this its colour may appear to an approaching gluon less if the gluon has large momentum, and large if it has less momentum. The coupling constant (or the interaction strength) depends on the energy scale; it is not a constant, but running. In the very high energy limit the coupling constant becomes very small, the quarks are non-interacting in the asymptotic limit! This is known as asymptotic freedom [8]. On the other hand in the low energy limit the coupling constant grows large. This is known as infrared slavery. Converting momentum scales to the length scales we may say that quarks are non-interacting at small distance scales and very strongly interacting at large distance scales. The quarks inside the nucleon are almost free, however, they interact very strongly if we try to bring one of them out of the nucleon. This explains scaling behavior in deep inelastic scattering, and justifies the confinement hypothesis.

Quantum chromodynamics possesses another interesting symmetry. Particles with zero mass move with the speed of light. If the alignment of spin and momentum (called helicity) of a mass less fermion is fixed in one frame it will appear same from all other frames as no frame can move faster than it. Thus helicity of a mass less particle is conserved. It is associated with a symmetry called chiral symmetry. Masses of u, d and s quarks, that constitute the low lying excitations of strong interaction physics, are small compared to the energy scale of QCD, m_u 2 MeV, m_d 5 MeV and m_s 140 MeV In the limit, m_u, m_d, m_s 0, quark dynamics has chiral symmetry (though explicitly broken to a small extent). However, when these quarks form a nucleon they acquire mass of about 350 MeV (1000 MeV/3), consequently the chiral symmetry is lost. This situation where the symmetry possessed by the dynamics is lost in the ground state is called spontaneous symmetry breaking. The consequence of spontaneous symmetry breaking is that the ground state hosts mass less bosonic excitations called ``Goldstone Bosons'' [9]. Thus, the chiral symmetry is spontaneously broken in QCD, and the massless Goldstone bosons are the spin zero negative parity octet mesons, namely ($^+$, ^{0}, $^-$, , K^+, K^-, K^0, K^0). The order parameter associated with chiral symmetry breaking is the so-called chiral or quark condensate. The spontaneous chiral symmetry breaking implies that a massless (or nearly massless) quark develops a non-zero dynamical mass. interacting with the quark condensates. The Goldstone bosons become the fundamental degrees of freedom of low energy QCD. Small masses of these Goldstone bosons is due to the fact that the chiral symmetry was not exact but explicitly broken by a small amount

Spontaneous symmetry breaking is a widespread phenomenon, and analogues exist in various other areas of physics. In case of paramagnetic to ferromagnetic transition the basic hamiltonian of this spin system is invariant under rotations in space. However, its low temperature phase is characterized by a non-vanishing magnetization which points into a definite direction in space. Rotational symmetry is spontaneously broken. This is a non-perturbative, collective phenomenon. Many spins cooperate to form the macroscopically magnetized material. Slow variations in the direction of the magnetization produce a collective low-frequency, long wavelength motion of the spins. This spin wave (magnon) is the Goldstone boson of spontaneously broken rotational symmetry. In case of spontaneous chiral symmetry breaking, the analogue of the non-vanishing magnetization is the chiral condensate; the analogue of the spin wave is the octet mesons.

The main features of QCD that percolate to low energy strong interaction physics:

There are two vacuua called perturbative vacuum and physical vacuum. Perturbative vacuum hosts colored quarks and gluons, but physical vacuum hosts color-less hadrons in which quarks are confined.

Chiral symmetry is spontaneously broken in transition from perturbative to physical vacuum. Perturbative vacuum is chiral symmetric, as u, d, s quarks are almost mass-less and physical vacuum is not because quarks acquire mass.

Any model trying to understand strong interaction at low energy must take into account the above two features to be consistent with the fundamental theory of strong interaction.

Free Baryons and Resonances

Formation of structure in low energy QCD can be addressed by studying the complete spectrum of excited states of nucleon. This includes the determination of the quantum numbers and decay branching ratios of the excited states as well as the extraction of the couplings of the states to interaction probes.

QCD is established as a fundamental theory of the strong interaction. In principle, one should be able to construct strongly interacting particles and their interaction starting from QCD. However, realization of QCD towards this goal has not yet been achieved completely. This is mainly because of the fact that quark gluon coupling constant (or interaction strength) becomes large at low energy, and consequently perturbative techniques fail. Numerical methods, requiring huge resources, are being tried and considerable progress has been made there.

In this situation, QCD inspired models have been introduced to understand baryons and resonances. There are two classes of models. In one class, quarks are taken as the basic degrees of freedom, which are confined by a potential put by hand. The feature of spontaneous breaking of chiral symmetry has been considered in these models. This model and its several variants are known as constituent quark model [10]. In another class of models spontaneous breaking of chiral symmetry is taken as the fundamental feature of low energy QCD. The basic degrees of freedom here are the Goldstone bosons, and baryons emerge as the solitonic excitation of the non-linear interaction among the Goldstone bosons. These models are known as chiral soliton models [11].

Experimentally general features of the excitation energy spectrum of the nucleon, and the properties of most of the baryon resonances have been determined from pion elastic and inelastic scattering. The baryon spectrum can be fairly well accounted for by constituent quark model taking three dimensional spin-independent harmonic oscillator potential as the confining potential. However, for a more detailed description of the excitation energy spectrum a spin dependent quark-quark interaction has to be included. The spin dependent potential can be generated through one gluon exchange or scalar meson exchange between the quarks [12].

Baryons and Resonances in Nuclei

When baryonic or mesonic resonances form in side nucleus by photo excitation or strong interaction processes, the properties of the resonances are modified. It might be naively expected that any resonance structure would be broadened in a nucleus due to many body effects comprising of Fermi motion, collisional broadening (N*N N*N) and additional decay modes (N*N NN). These channels are not available for free baryon resonances. Resonance excitation in nuclei, however, also will be narrowed by medium effects due to Pauli blocking final states. For example, the decay, N is prohibited if the final state of the nucleon is occupied.

However, modification of the properties of hadrons including resonances can occur inside the nuclear medium due to a fundamental feature of QCD. The order parameter of the spontaneous chiral symmetry breaking, the quark condensates, may change inside the nuclear medium. Model calculations show that quark condensate decreases with increasing density and temperature of the medium, leading to partial restoration of chiral symmetry inside nuclear medium. Thus, in the nuclear medium quarks are expected to have lower constituent mass than that in a free nucleon. The

hadron masses may be lowered inside the nuclear medium. The meson-nucleon interaction strength also will be modified.

Experimental signatures towards this are looked for in di-lepton ($e^+ e^-$) spectrum in heavy ion collisions [13]. Di-leptons are mostly the decay products of vector (spin =1) meson, such as rho meson. Modification of rho meson mass inside the nuclear medium would lead to the shift of peak in dilepton spectrum and signal partial restoration of chiral symmetry in nuclear medium. Experiments have not been able to identify yet clearly the effect arising from the chiral restoration in nuclear medium.

Pentaquark

There are many possibilities for combining quarks with color into colorless hadrons. However, only two configurations of the usual mesons and baryons have been found till now, though QCD predicts the existence of mesons and baryons with more complicated internal structure. The non-conventional mesons could be made of a quark, anti-quark and one gluon, ($q\bar{q}g$) called hybrid, or of three gluons, (qqg) called glueballs, or of two quarks and two antiquarks, ($qqq\bar{q}$) , etc. Similarly non-conventional baryons could be made of three quarks and a gluon, ($qqqg$), or four quarks and an antiquark ($qqqq\bar{q}$), etc.

Baryons whose minimum quark content is four quarks and one antiquark are called ``pentaquarks'', and those in which the antiquark has a different flavor than the other four quarks are called ``exotic'' pentaquarks. The quantum number for these states cannot be defined by only three quarks. For example, in non-exotic (uudss), baryon number, B= 1/3 + 1/3 + 1/3 + 1/3 - 1/3 = 1 and strangeness, S= 0 + 0 + 0 + -1 + 1 = 0; and for exotic (uudd$\bar{s}$), baryon number = 1/3 + 1/3 + 1/3 + 1/3 - 1/3 = 1 and strangeness = 0 + 0 + 0 + 0 + 1 = 1. A baryonic state with S = +1 is explicitly exotic, and observation of such a state opens up new direction in strong interaction physics.

There were searches in the 1960's and 1970's mostly in bubble chamber experiments with incident and K beams for a baryon with positive strangeness. Those experiments found no enhancements in S = +1 baryon channels.

Mass of (uudd$\bar{s}$) pentaquark (called $^+$) with spin = 1/2, isospin = 0, parity = +, strangeness = 1, was predicted about 1800 MeV, and width around hundreds of MeV in the constituent quark model. However, chiral soliton model [15] predicted mass and width of $^+$ as 1530 MeV and about 15 MeV respectively. The width prediction was the key for the revival of experimental search for $^+$, and in 2003 first observation was claimed in photo-production on bound neutron in ^{12}C, + n $^+K^-$ K^+nK^-. The invariant mass spectra of, K^+n, shows a clear peak at, 1540 10 MeV.

However, observation of $^+$ is controversial yet, as some experimental groups did not confirm its own discovery. It is widely believed that pentaquarks ``do not exist''. In recent experiments, it is again observed. More experiments are planned.

If the existence of pentaquark is confirmed it will change our view on strong interactions. Firstly, quark model and its variants will be proved to be incomplete and should be revisited for several reasons. The traditional view of hadrons as "made of" constituent quarks with mass ~350 MeV, cannot explain its low mass and width. The constituent quark models ignored two important features of QCD namely, (1) according to quantum field theory baryons are actually superposition of states with 3, 5, 7,…quarks, and (2) that constituent quarks have to interact strongly with pion and kaon fields due to spontaneous breaking of chiral Symmetry.

Summary

A tricky point in nuclear physics, known for a long time, is that the nucleons and mesons, the usual hadorns that are observed in the asymptotic states are not the basic degrees of freedom of the strong interaction that governs the dynamics. The fundamental degrees of freedom of strong interaction are quarks, and the interaction of these quarks is described by QCD in terms of exchange of gluons between them. Hadrons are colorless composites of quarks and low-lying excitations in the QCD vacuum. The QCD vacuum, in which hadronic excitations are built, thus, is not the perturbative vacuum; also, this vacuum does not

share some of the symmetries of QCD, the chiral QCD is not manifest in the physical vacuum. The chiral symmetry of QCD is spontaneously broken. Chiral symmetry of QCD and its spontaneous breaking play a very important role in understanding the strong interaction dynamics at low energy.

Nuclei exhibit a very rich excitation spectrum. By studying these excitation spectrum it is possible to identify the correct low energy behavior of QCD, the fundamental theory of strong interaction.

References

1. H. L. Anderson et al., Phys. Rev.85 (1952) 934
2. Gell-Mann, M. and Neeman, Y. The Eightfold Way (W.A. Benjamin Inc.) (1964).
3. M. Gell-Mann, Phys. Lett. 8 (1964)214; G. Zweig, CERN report No. 8182 TH 401 (1964).
4. J. I. Friedman, R. W. Kendal, Ann. Rev. Nucl. Sci, 22 (1972) 203.
5. J.D. Bjorken, Phys. Rev. 179 (1969) 1547: R.P.Feynman, Phys. Rev. Lett. 23 (1969) 1415
6. M. Gell-Mann, Acta Phys. Austriaca Suppl. 9 (1972) 733; M. Han and Y. Nambu, Phys. Rev. 139B (1965) 1006.
7. H. Fritzsch, M. Gell-Mann and H. Leutwyler, Phys. Lett. 47B (1973) 365.
8. D.J. Gross and F. Wilczek, Phys. Rev. Lett. 30 (1973) 1343, H.D. Politzer, Phys. Rev. Lett. 30 (1973) 1346.
9. J. Goldstone, Nuov. Cim. 19 (1961) 154.
10. A. Chodos, R. L. Jaffe, K. Johnson, C. B. Thorn, V. Weisskopf, Phys. Rev.D9 (1974)3471; A. Chodos, R. L. Jaffe, K. Johnson, C. B. Thorn Phys. Rev.D10 (1974)2599
11. T. H. R. Skyrme, Proc. Royal Soc. A260 (1961)127; Nucl. Phys. 31(1962)556.
12. Ya. Glozman, D.O.Riska, Phys. Rep. 268 (1996) 263
13. G. Agakichiev et al, CERES Collaboration, Phys. Lett. B 422, 405 (1998)
14. R. L. Jaffe, Phys.Rev.D15:267,1977, Phys.Rev.D15:281,1977
15. D. Diakonov, V. Petrov and M. Polyakov, Z. Phys. A 359(1997) 305
16. T Nakano et al, Phys. Rev. Lett. 91 (2003) 012002